Graduate School ETD Form 9
(Revised 12/07)

PURDUE UNIVERSITY
GRADUATE SCHOOL
Thesis/Dissertation Acceptance

This is to certify that the thesis/dissertation prepared

By Subramanian Dharmarajan

Entitled
BMP Pathway and Reactive Retinal Gliosis

For the degree of Master of Science

Is approved by the final examining committee:

Dr. Teri Belecky-Adams
Chair

Dr. David Skalnik

Dr. Xin Zhang

To the best of my knowledge and as understood by the student in the *Research Integrity and Copyright Disclaimer (Graduate School Form 20)*, this thesis/dissertation adheres to the provisions of Purdue University's "Policy on Integrity in Research" and the use of copyrighted material.

Approved by Major Professor(s): Dr. Teri Belecky-Adams

Approved by: Dr. Simon Atkinson 07/13/2012
Head of the Graduate Program Date

Graduate School Form 20
(Revised 9/10)

PURDUE UNIVERSITY
GRADUATE SCHOOL

Research Integrity and Copyright Disclaimer

Title of Thesis/Dissertation:

BMP Pathway and Reactive Retinal Gliosis

For the degree of Master of Science

I certify that in the preparation of this thesis, I have observed the provisions of *Purdue University Executive Memorandum No. C-22,* September 6, 1991, *Policy on Integrity in Research.**

Further, I certify that this work is free of plagiarism and all materials appearing in this thesis/dissertation have been properly quoted and attributed.

I certify that all copyrighted material incorporated into this thesis/dissertation is in compliance with the United States' copyright law and that I have received written permission from the copyright owners for my use of their work, which is beyond the scope of the law. I agree to indemnify and save harmless Purdue University from any and all claims that may be asserted or that may arise from any copyright violation.

Subramanian Dharmarajan

Printed Name and Signature of Candidate

07/13/2012

Date (month/day/year)

*Located at http://www.purdue.edu/policies/pages/teach_res_outreach/c_22.html

BMP PATHWAY AND
REACTIVE RETINAL GLIOSIS

A Thesis

Submitted to the Faculty

of

Purdue University

by

Subramanian Dharamarajan

In Partial Fulfillment of the

Requirements for the Degree

of

Master of Science

August 2012

Purdue University

Indianapolis, Indiana

ACKNOWLEDGEMENTS

I wish to express my gratitude towards my advisor, Dr. Teri Belecky-Adams, for all the support, encouragement and guidance, as well as her delicious brownies and rice krispie treats. You have helped me become the researcher I am today. To my committee members, Dr. Xin Zhang and Dr. David Skalnik, I appreciate your insight and assistance throughout my project. I would like to thank the Belecky-Adams lab for their friendship and support throughout my time here. I would also like to thank my parents. They were always supporting and encouraging me with their best wishes.

TABLE OF CONTENTS

Page

Page

LIST OF TABLES

LIST OF FIGURES

Figure Page

LIST OF ABBREVIATIONS

Aggrecan	ACAN
Bone morphogenic proteins	BMP
Central nervous system	CNS
Chondroitin sulfate proteoglycans	CSPG
Cycle threshold	C_T
Epidermal growth factor receptor	EGFR
Fibroblast growth factor	FGF
Glial fibrillary acidic protein	GFAP
Glutamine synthetase	GS
Immunohistochemistry	IHC
Inhibitor of differentiation	ID
Matrix metalloproteinases	MMP
N-methyl-D-aspartic acid	NMDA
Neurocan	NCAN
Nitric oxide synthase	NOS
Phosphacan	PCAN
Phosphate buffer saline	PBS
Phospho SMAD	pSMAD
Real time quantitative polymerase chain reaction	RT-qPCR
Ribonucleic acid	RNA

Sonic hedgehog	SHH
Tissue inhibitor of metalloproteinases	TIMP
Toll like receptor	TLR
Transforming growth factor	TGF
Tris buffered saline-tween	TBST
Versican	VCAN
Vimentin	VIM
Wild type	WT

ABSTRACT

Dharmarajan, Subramanian. M.S., Purdue University, August 2012. BMP Pathway and Reactive Retinal Gliosis. Major professor: Teri Belecky-Adams.

Reactive gliosis is known to have a beneficial and a degenerative effect following injury to neurons. Although many factors have been implicated in reactive gliosis, their role in regulating this change is still unclear. We investigated the role of bone morphogenetic proteins in reactive gliosis *in vivo* and *in vitro*. *In vivo*, IHC analysis indicated reactive gliosis in the 6 week $Ins2^{Akita}$ mouse and WPK rat retinas. Expression of BMP7 was upregulated in these models, leading to an increase in the phosphorylation of downstream SMAD1. *In vitro*, treatment of murine retinal astrocyte cells with a strong oxidizing agent such as sodium peroxynitrite regulated RNA levels of various markers, including GFAP, CSPGs, MMPs and TIMPs. BMP7 treatment also regulated RNA levels to a similar extent, suggesting reactive gliosis. Treatment with high glucose DMEM and BMP4, however, did not elicit increase in levels to a similar degree. Increase in SMAD levels and downstream targets of SMAD signaling such as ID1, ID3 and MSX2 was also observed following treatment with sodium peroxynitrite *in vitro* and in the 6 week $Ins2^{Akita}$ mouse retinas *in vivo*. These data concur with previously established data which show an increase in BMP7 levels following injury. It also

demonstrates a role for BMP7 in gliosis following disease. Further, it suggests SMAD signaling to play a role in initiating reactivity in astrocytes as well as in remodeling the extracellular matrix following injury and in a disease condition.

CHAPTER 1 INTRODUCTION

Nervous system and its development

The formation of the nervous system begins at the gastrula stages of embryonic development. At this stage, the 3 germinal layers of the embryo: ectoderm, endoderm and mesoderm, have been specified. A specialized group of cells termed the organizer signal the development of the nervous system in the ectoderm. The first step in the development of the nervous system is termed neural induction. Signals from the organizer are interpreted by competent cells, which then are committed to becoming neural stem or precursor cells, which will give rise to all the cells of the central and peripheral nervous system. Once the cells become committed, the precursor cells differentiate into the appropriate neural cell type based on intrinsic and extrinsic cues during development.

Initial studies in amphibian embryos showed that the default pathway of ectoderm cells is to differentiate into neural cells. Studies using *Xenopus laevis* embryos showed that expression of the bone morphogenetic protein (BMP) molecule prevented the neural fate, and induced an epidermal fate (Wilson and Edlund, 2001). During gastrulation, inhibitors of the BMP molecule are secreted by the organizer and mesoderm, which blocks the effects of BMP and allow the

cells to proceed towards a neural fate. Further, signaling molecules such as Wnts – which help establish the initial dorso-ventral polarity of the embryo and fibroblast growth factor (FGF), have also been implicated in neural induction (Fig. 1) (Wilson and Edlund, 2001). This thickened region of ectoderm which consists of neuroepithelium is termed the neural plate (Weinstein and Hemmati-Brivanlou, 1999, Wilson and Edlund, 2001).

Following neural induction, the next step is neurulation which is the formation of the neural tube that ultimately gives rise to the different parts of the nervous system. Primary neurulation as stated in a review by Greene, N.D.E. and Copp, A.J., 2009, is “the shaping and folding of the neural plate which undergoes fusion in the midline to generate a neural tube. Secondary neurulation is the formation of the neural tube in the regions of the future caudal spine” (Greene and Copp, 2009). Following the closure of the neural tube, organizing signals pattern the neural tube. This confers positional identity to the different progenitor domains, which give rise to the different neural and glial cell types under the influence of spatial and temporal mechanisms. Signals such as sonic hedgehog (SHH), fibroblast growth factor (FGF), Wnts, BMP and retinoic acid (RA) help pattern the neural tube (Fig. 2) (Harrington et al., 2009).

Glial cells, development and types

Glial cells are the neuron supporting cells found throughout the central nervous system (CNS) which vastly outnumber the neurons. In the developing nervous system, gliogenesis follows neurogenesis. They arise from the neuroepithelial precursor cells which give rise to neurons first, followed by a fate switch step which then restricts them to generate the glial cells (Fig. 3). Signals such as SHH, BMP and FGF play a role in the differentiation of the glial cells from the neuroepithelial precursor cells. The JAK-STAT pathway and the Notch signaling pathway also play a role in gliogenesis (He and Sun, 2007). The two major types of the macroglial population include the astrocytes and the oligodendrocytes. The precursor cells give rise to the astrocytes first and then the oligodendrocytes (Rowitch and Kriegstein, 2010).

Astrocytes: Functions and types

The astrocytes are the star shaped population of the glial cell type. These cells are broadly classified into fibrous and protoplasmic astrocytes. Fibrous astrocytes are found in the white matter and exhibit a star like morphology, while the protoplasmic astrocytes are found in the grey matter and exhibit a complex morphology with frequently branching processes (Levison, 2005, Sofroniew and Vinters, 2010). In another approach to classify astrocytes based on studies of the morphology, antigen presentation and response to growth factors, astrocytes are categorized into type I and type II (Levison, 2005). The type I astrocytes arise directly from the neuroepitheial precursor cells while the type II astrocytes arise

from a bipotent progenitor cell type: the oligodendrocyte-type II astrocyte (O-2A) precursor cell (Levison, 2005, Rompani and Cepko, 2010).

The astrocyte cells were initially thought to have supportive role in the nervous system, serving as “glue” holding the components together. However, studies over the past 20 years have shown these cells to be largely dynamic, interactive and perform a wide range of functions (Sofroniew and Vinters, 2010). During development, they serve as scaffolding molecules which aid in the migration of axons. Synapses in the nervous system usually have astrocytes associated with them. Studies have shown that astrocytes play a role in the maturation of functional synapses via secretion of various factors (Allen and Barres, 2005, He and Sun, 2007). At the synapse, the astrocytes help in uptake of ions and neurotransmitters as well as play an active role in increasing synaptic activity (Pfrieger and Barres, 1997, Barres, 2008). Regulation of calcium levels in astrocytes affects synaptic transmission by regulating release of molecules such as ATP, GABA and glutamine (Barres, 2008, Sofroniew and Vinters, 2010). Astrocytes also have been shown to have connections with blood vessels (Gordon et al., 2007, Sofroniew and Vinters, 2010). These studies have shown that astrocytes play a role in regulating blood flow by releasing mediators such as arachidonic acid and nitric oxide. The end feet of the astrocytes found in close association with the endothelial cells aiding the formation of tight junctions in these cells, forming the blood brain barrier (Abbott et al., 2006). They also play a role in energy and metabolism, by serving as a nutrient conduit between blood

vessels and neurons as well as storing energy in the form of glycogen (Sofroniew and Vinters, 2010).

Development of the eye

The vertebrate eye develops from the eye field in the anterior neural plate. The neural plate initially folds upwards and inwards forming the neural tube. The eye field then splits forming initially the optic grooves, which then evaginate and forms the optic vesicles. The optic vesicle divides or separates into the neural retina, retinal pigmented epithelium and the optic stalk. The optic vesicles evaginate, coming in close proximity of the head ectoderm. Signals arising from the evaginating head ectoderm induce the formation of the lens placode from a thickened region of the head ectoderm called the lens placode (Fuhrmann, 2010). The lens placode eventually gives rise to the lens. The optic vesicle now folds on itself, with the layer close to the lens placode becoming the neural retina and the layer distal to the placode becoming the retinal pigmented epithelium. The optic stalk which is the most proximal part of the vesicle narrows to become the optic fissure, through which the optic nerve leaves the eye (Lamb et al., 2007, Fuhrmann, 2010) (Fig. 4).

Retina and glial cells

The mature retina can be divided into 6 layers namely the outer and inner nuclear layers, the outer and inner plexiform layers, the ganglion cell layer and

the nerve fiber layer (Cheng et al., 2006) (Fig. 5). These layers are primarily made of neuronal cell types and include: rod and cone photoreceptor, the bipolar interneurons, and horizontal and amacrine cells. The retina has 2 major types of glial cells – the Muller glial cells and the retinal astrocyte cells (Bringmann et al., 2006).

Muller glial cells arise from the multipotent retinal progenitor cells. Birthdating studies have shown that the progenitor cells give rise to ganglion cells first, followed by horizontal cells and cones and lastly amacrine cells, bipolar cells, rods and muller glial cells (development of retina and optic pathway paper). They arise following terminal differentiation of the progenitor cells under the influence of notch signaling. The cell bodies are present in the inner nuclear layer with the process extending through the retina to the outer limiting membrane that divides the photoreceptor inner and outer segment from the cell body and the outer limiting membrane that divide the retina from the vitreous. The Muller glial cells play an important role in maintaining structure and function in retina, apart from the functions previously mentioned (Dubois-Dauphin et al., 2000, Bringmann et al., 2009, Jadhav et al., 2009).

Retinal astrocytes are present in the optic nerve, optic nerve head and the retinal nerve fiber layer with the processes extending into the ganglion cell layer (Huxlin et al., 1992). The developing eye expresses factors such as Pax2 and Pax6, all through the optic vesicle stage. As development proceeds, expression of Pax2 is

restricted to cells of astrocytic lineage (Chu et al., 2001). The retinal astrocytes are generated in the optic stalk from the neuroepithelial precursor cells and then migrate into the retina. Development of glial cells in the optic stalk is mediated by signals from the retinal ganglion cells, which includes sonic hedgehog (SHH) and BMP7 (Watanabe and Raff, 1988, Huxlin et al., 1992, Morcillo et al., 2006, Dakubo et al., 2008). These retinal astrocytes play an important role in establishing the retinal vasculature (Kuchler-Bopp et al., 1999).

Reactive astrocytes

An important property of astrocytes is their response to any damage/injury to nearby neurons; a response known as reactive gliosis. Although there is no clear definition for reactive astrogliosis, based on the large number of studies on reactive astrocytes, reactive astrogliosis can be defined as: “The changes in molecular and morphological characteristics of astrocytes due to an injury or disease of the nearby neurons, which alters the functions of astrocytes on a context dependent manner by inter and intra cellular signaling molecules, based on the severity of the disease or injury” (Ridet et al., 1997, Sofroniew, 2009, Sofroniew and Vinters, 2010) (Fig. 6). Several different transcriptional regulators such as NF – κB, STAT3 and mTOR are regulated during reactive gliosis (Brambilla et al., 2005, Herrmann et al., 2008, Codeluppi et al., 2009, Sofroniew, 2009). Growth factors and cytokines such as fibroblast growth factor, epidermal growth factor and interleukins seem to be upregulated during the reactive state

(Eddleston and Mucke, 1993, Ridet et al., 1997, Gris et al., 2007, Sofroniew, 2009).

Many signaling molecules are able to induce reactive astrogliosis including: growth factors and cytokines such interleukins (IL), ciliary neurotrophic factor (CNTF), transforming growth factor β (TGF-β), interferon-gamma (IF) , immunity mediators such as toll like receptors and lipopolysaccharides, neurotransmitters, reactive oxygen species like nitric oxide and molecules associated with metabolic toxicity and neurodegeneration such as ammonia and β-amyloid (Sofroniew, 2009, Sofroniew and Vinters, 2010). These signals either on their own or in combination with different molecules, alter the characteristics of astrocytes in reactive astrogliosis. The signaling mechanisms regulated depend on the type of stimulus and this controls the severity of reactive astrogliosis. Broadly, the reactive astrogliosis can be grouped into: (1) Moderate to mild reactive astrogliosis – hypertrophy and variable upregulation of expression of GFAP without overlap of processes of neighboring astrocytes, (2) severe diffusive astrogliosis – marked upregulation of glial fibrillary acidic protein (GFAP) and other genes, along with hypertrophy and proliferation of astrocytes leading to overlapping of processes with neighboring cells, and (3) severe astrogliosis with glial scar – show characteristics of either sever diffusive or milder astrogliosis along with the formation of a physical neuroprotective barrier, termed as the glial scar (Sofroniew and Vinters, 2010).

The primary function of reactive astrogliosis is to aid in neural protection by preventing the spread of the injury in the CNS and minimizing tissue damage and lesion size. Studies over the past two decades using various animal models have shown that reactive gliosis aids in protection from oxidative stress, blood brain barrier repair, stabilizing extracellular fluid and ion balance and reducing edema, and also in limiting the spread of inflammatory cells (Bush et al., 1999, Myer et al., 2006, Voskuhl et al., 2009, Sofroniew and Vinters, 2010). During gliosis, the astrocyte function is altered. They hypertrophy due to an increased accumulation of intermediate filaments, remodel the extracellular matrix leading to scarring, and release neuroprotective and/or cytotoxic molecules, by regulating the expression of various molecules and enzymes (Sofroniew, 2009). A number of markers have been identified over the years which can specifically identify astrocytes. The expression of the intermediate filament – GFAP, is often used as a major identifying marker of astrocytes and its upregulation during gliosis has been often used a criteria to detect reactivity (Levison, 2005). Another intermediate filament which is upregulated during gliosis is vimentin (Yang and Hernandez 2003). Astrocytes also express S100 – β, which is a calcium binding protein involved in various intra and inter cellular processes. Glutamine synthetase, which is an enzyme involved in glutamate recycling is also specific to astrocytes (Hertz and Zielke, 2004). Nitric oxide synthase, an enzyme involved in the synthesis of nitric oxide, has also been previously observed to be regulated during gliosis (Cassina et al., 2002a). During reactive gliosis, expression of these

markers has been observed to be upregulated (Ridet et al., 1997, Sofroniew, 2009).

Reactive gliosis also leads to the formation of a glial scar, brought on by remodeling of the extracellular matrix. Various knowckout and knockdown studies have shown that the presence of reactive gliosis is in fact a positive effect in the early stages. Studies of glial scars using double GFAP -/- vimentin -/- mice and mice expressing a GFAP-herpes simplex virus (Pekny et al., 1999, Faulkner et al., 2004) showed in the two injury models that ablation of astrocytes led to a more severe and marked damage of the neurons and oligodendrocytes (Renault-Mihara et al., 2008).The primary negative effect of reactive astrogliosis is the long term persistence of the glial scar, which contain the inhibitory chondroitin sulphate proteoglycans (CSPGs) that prevent axonal regeneration.

Remodeling of the extracellular matrix, ultimately leading to the formation of a glial scar, is mediated primarily by the regulation of CSPGs and the enzymes matrix metalloproteinases (MMPs) (Silver and Miller, 2004, Crocker et al., 2006). The CSPGs belong to a larger class of molecules, termed the proteoglycans, which also includes heparin sulfate proteoglycans (HSPGs), keratin sulfate proteoglycans (KSPGs) and dermatan sulfate proteoglycans (DSPGs). The HSPGs primarily help in stabilizing extracellular interactions between receptor and its ligand. The CSPGs, however, act mainly as “barrier molecules” that restrict migration, growth and plasticity of neurons (Laabs et al., 2005). During

gliosis, these inhibitory CSPGs such as neurocan, phosphacan, aggrecan and versican are upregulated, which inhibit axonal regrowth (Silver and Miller, 2004, Laabs et al., 2005). Studies have shown regenerating neurons are repulsed by the presence of these inhibitory CSPGs, reducing the ability for axonal regeneration (Rhodes and Fawcett, 2004). Further, injecting chondroitinase (an enzyme which degrades the GAG chain of proteoglycans) at the site of injury, leads to a decrease in scar formation and an increase in axon regeneration (Zuo et al., 1998). The HSPGs, however, have been found to be both stimulating and inhibitory to axonal regrowth (reviewed in Pizzi and Crowe, 2007).

Another set of molecules involved in extracellular matrix remodeling are the MMPs and their tissue inhibitors (TIMPs). Over 20 different MMPs have been identified and the main function of these enzymes is to help remodel the extracellular matrix by degrading the extracellular matrix (Nagase et al., 2006). As summarized in a review by Pizzi MA and Crowe MJ (2007), the MMPs can be regulated (1) at the transcriptional level, (2) by the activation of the precursor zymogen or (3) by the TIMPs (Pizzi and Crowe, 2007). The MMPs target a wide range of ECM molecules, including the CSPGs. Particularly, MMP-2 and -9 have been shown to degrade the inhibitory CSPG neurocan as well as CD-44 (Tucker et al., 2008). In a study using the healer mouse model, increase in RNA levels of MMP -2 and -9 along with an increase in MMP-14 lead to an increase in the degradation of neurocan and CD-44, thereby, decreasing scarring (Tucker et al., 2008). However, increase in the levels of MMPs and TIMPs have been linked to

various neurodegenerative such as parkinson's disease, cerebral ischemia and spinal cord injuries, as well as in neuroinflammatory responses following hypoxia and cerebral ischemia (Rosenberg, 2002, Crocker et al., 2006), which can indirectly alter the extracellular matrix. During gliosis, the normal balance between the MMPs and TIMPs and also other components of the ECM is dysregulated and this may lead to scaring (Laabs et al., 2005, Tucker et al., 2008).

Reactive gliosis in the eye and optic nerve

The astrocytes of the retina, optic nerve and optic nerve head become reactive in various disease states such as glaucoma and retinal ischemia (Hernandez et al., 2008). When the astrocytes become reactive, as stated before, they increase GFAP expression and hypertrophy. However, the proliferative response of reactive astrocytes in the eye is still unclear. Contradictory results were observed when Inman et al. 2007, observed non proliferative reactive astrocytes in a mouse model of glaucoma, while Johnson et al. 2000, observed proliferative reactive astrocytes in a rat model of glaucoma. Nevertheless, reactive astrocytes begin to express various cytokines such as tumor necrosis factor- α (TNF-α) and interleukins (IL) among others, which promote the death of the retinal gangion cell (RGC) axons (Yuan and Neufeld, 2000, Nakazawa et al., 2006). Other mechanisms implicated in the death of retinal ganglion cells are reactive oxygen species and nitric oxide (Levin, 1999, Neufeld et al., 1999). Reactive astrocytes in the optic nerve form cribriform structures and migrate from these structures to

the nerve fibers where they synthesize the neurotoxic substances (Liu and Neufeld, 2004). Thus, retinal gliosis serves to protect and repair retinal neurons.

The Bone Morphogenetic Proteins - BMP's

The bone morphogenic proteins (BMPs) consist of a large number of signaling molecules belonging to the transforming growth factor-β (TGF-β) superfamily (Hogan, 1996). With more than 20 members, the BMPs are involved in a wide range of functions including embryonic development, neural patterning, limb patterning, skeletal development and organogenesis of the kidney, lung and eye (Hogan, 1996). The BMP ligand molecules signal primarily by forming dimers, which then bind to the receptors associated proteins. The BMP receptors are serine threonine kinase receptors, classified into 2 groups: the type I and type II receptors. The BMP type I receptors act downstream of the type II receptors and determine the specificity of the signal (Conidi et al., 2011). Three type I (Alk -2, -3 and -6) and type II (BMPRII, ActR II A and ActR II B) receptors have been identified which bind BMP ligands (Nohe et al., 2004, Miyazono et al., 2010). Binding of the ligand leads to phosphorylation and activation of the receptors, which then phosphorylate the receptor, bound signaling mediators.

The primary receptor bound mediators of BMP signaling include the receptor SMADs (SMAD -1, -5 and -8), x-linked inhibitor of apoptosis (XIAP) protein and the immunophilin FKBP12 (Rajan et al., 2003, Nohe et al., 2004, Miyazono et al., 2010).

- Activation of the receptor leads to phosphorylation of the receptor SMADs. The phosphorylated SMADs dimerize with SMAD4 which is then translocated to the nucleus and binds to specific sequences in the DNA bringing about transcriptional regulation of target genes by either directly binding them and/or through association with other DNA binding factors (Nohe et al., 2004). This pathway is negatively regulated through the inhibitory SMAD molecules SMAD -6 and -7 (Nakayama et al., 1998, Zhu et al., 1999).
- XIAP has been found to interact with Alk-3 and TAB1 (which activates a member of the MAP kinase kinase kinase family – TAK1) (Yamaguchi et al., 1999, Nohe et al., 2004, Bond et al., 2012). Signaling via XIAP leads to the formation of a XIAP-TAB1-TAK1 complex, activating the MAPK pathway (Sieber et al., 2009)
- The molecule FKBP12 has been found to be associated with Alk3 (Nohe et al., 2004). Phosphorylation of the FKBP12 protein activates the FRAP (FKBP12 rapamycin associated protein) molecule which then activates the FRAP-STAT signaling mechanism (Rajan et al., 2003).

The BMP signaling proceeds through the canonical SMAD dependent pathway; and/or the non-canonical SMAD independent pathway to bring about a change at the gene transcriptional level (Baker and Harland, 1997, Derynck and Zhang, 2003, Herpin and Cunningham, 2007, Bragdon et al., 2011) (Fig. 7). Further, the

BMPs also signal via a non-transcriptional mechanism by regulating various molecules such as micro RNAs (miRNA) and phopho-inositol 3 kinase (PI3K) (Ghosh-Choudhury et al., 2002, Qin et al., 2009, Sieber et al., 2009).

BMPs play a key role in the development of the nervous system. Early in development, BMP-4 and -7 are expressed in the ectoderm. Blocking of the BMP signaling in the ectoderm cells leads to the induction of the neural ectoderm. The region in which BMP signaling is not blocked is induced into the epidermis. Following neural induction, within the neural tube, the BMP molecules (BMP-2, -4, -5, -6 and -7) serve as a gradient morphogen regulating the development of the dorsal cell types. Further down in development, BMPs regulate astrogliogenesis during brain maturation (Mehler et al., 1997). They can serve as morphogens mediating long range signaling or act as short range signaling molecules by mediating cell to cell signaling (Mehler et al., 1997).

BMP molecules are essential for the morphogenesis of the eye (Luo et al., 1995, Jena et al., 1997, Wawersik et al., 1999, Furuta, 2000, Belecky-Adams and Adler, 2001). The BMPs and their receptors have been implicated to have a major function in the developing as well as adult ocular tissues. In particular the patterning of the eye field, the optic nerve head and differentiation of lens placode and retinal pigmented epithelium depends on BMP7 (Dudley et al., 1995, Luo et al., 1995, Wawersik et al., 1999, Adler and Belecky-Adams, 2002). The BMPs have been implicated in the regulation of the astrocytic lineage in the brain

(Mehler et al., 1997). In the eye, optic nerve head astrocytes have been shown to express BMP7 (Zode et al., 2007).

BMP and CNS injury

Studies using various CNS injury models have shown that the BMP pathway is upregulated at the site of injury in the CNS. Specifically, BMP-2, -4 and -7 have been found to be upregulated at the site of injury in spinal cord lesions (Setoguchi et al., 2001, Hampton et al., 2007, Matsuura et al., 2008a, Ueki and Reh, 2012). These molecules are also implicated in astrogliogenesis from precursor cells (Mabie et al., 1997, Mehler et al., 2000). Studies looking into BMP expression in reactive astrocytes have primarily used a spinal cord injury model (Setoguchi et al., 2001, Enzmann et al., 2005, Matsuura et al., 2008b, Sahni et al., 2010, Xiao et al., 2010). These studies have shown the regulation of BMP 4 and 7 as well the BMP inhibitor noggin, at the site of injury. These have primarily looked into the role of the BMPs in specifying a NG2+ astrocyte/oligodendrocyte progenitor following injury. These studies have shown inhibiting BMP signaling can either increase lesions following spinal cord injuries (Enzmann et al., 2005) or increase axonal regrowth (Matsuura et al., 2008a). Further, Sahni et al., 2010 showed that Alk-3 (BMPRIa) played a role in “reactive gliosis and wound closure” while Alk-6 (BMPRIb) increased glial scaring (Sahni et al., 2010). These studies indicate BMP signaling plays a role in both the advantageous and unfavorable effects of gliosis following spinal cord injury.

A recent study by Ueki and Reh looked at BMP signaling in the retina following N-methyl-D-aspartic acid (NMDA) induced retinal ganglion cell death and exposure to bright light. They observed an upregulation of BMP-2,-4 and -7 and phosphorylation of SMAD 1/5/8 following NMDA treatment or exposure to bright light, indicating that this response was a common reaction to retinal damage (Ueki and Reh, 2012).

Here, we hypothesize that the BMP pathway not only plays a role in initiating reactive gliosis in astrocytes of the retina, but is key to the extracellular matrix remodeling that occurs following injury and as well as during disease. We propose here that the BMPs, which are upregulated at the site of injury, play an active role in gliosis as well and not just in the specification of glia. As a first step to identify reactive astrocytes, degenerative retinal animal models were compared to their wild types for the expression of previously established reactive astrocyte markers. Using an *in vitro* retinal astrocyte cell line, effects of treatment with different concentrations of BMP-7 on the expression of various markers was analyzed. The animal models used for the study are the $Ins2^{Akita}$ diabetic mouse model and the Wistar (WPK) rat model. In these studies, we have shown the BMP levels increase in both model systems and that the muller glial cells and astrocytes respond to the BMP signal by increasing phospho-SMAD signaling. Further, when tested *in vitro*, BMPs were found to increase levels of molecules associated with reactive gliosis.

CHAPTER 2 MATERIALS AND METHODS

Tissue Processing and Fluorescence Immunohistochemistry

WPK rats were perfused through the left ventricle with 4% paraformaldehyde in 0.1M phosphate buffer. The eyes were dissected, fixed in 4% paraformaldehyde and incubated in an ascending series of sucrose (5%, 10%, 15% and 20%) made in 0.1M phosphate buffer, pH 7.4.The Ins2Akita eyes were dissected from the heads of euthanized animals, washed in PBS, and fixed in 4% paraformaldehyde. The eyes were then incubated in sucrose solution as previously mentioned. The tissues were frozen in a 3:1 20% sucrose-in phosphate buffer and OCT solution. 10 µm thick sections were cut using a Leica CM3050 S cryostat and placed on Superfrost Plus slide (Fisher Scientific, Pittsburgh, PA) treated with Vectabond (Vector Labs, Burlingame, CA), and were stored at -80°C until used for immunohistochemistry. For immunohistochemistry, sections were allowed to warm to room temperature for about 30-45 minutes, fixed with 4% paraformaldehyde for 30 minutes and incubated in methanol for 10 minutes at room temperature. Sections were then washed in 1X PBS subjected to antigen retrieval by placing the sections in 1% SDS (Fisher Scientific, Pittsburgh, PA) in 0.01 M PBS for 5 minutes and washed 3 times in 1X PBS. To aid in autofluorescence reduction, sections were treated with 1% sodium

borohydrite in PBS (Acros) for 2 minutes at room temperature, then rinsed with PBS. Tissue was blocked by incubating with 10% serum in 1X PBS containing 0.25% Triton X-100 (Biorad, Hercules, CA) at room temperature for 1 hour. The slides were incubated with the primary antibody, diluted in 0.025% TritonX-100 PBS with 2% blocking serum, overnight at 4°C. The following day, after 2 washes with 1X PBS, the slides were incubated in Dylight conjugated secondary antibody (Jackson Immunoresearch, West Grove, PA) at 1:800 diluted with 1X PBS, for 1 hour at room temperature, then washed twice with 1X PBS for 5 minutes each rinse, and mounted with ProLong Gold with DAPI (Invitrogen, Grand Island, NY). For labeling of mouse tissue slides with glutamine synthetase, blocking and overnight incubation with primary antibody was performed as specified by the Vector mouse on mouse immunodetection kit (Vector Labs, Burlingame, CA). For immunolabelling with neurocan and pSMAD1, following overnight incubation with the primary antibody, the sections were first incubated with biotinylated anti sheep/goat antibody (1:1000, Vector Labs, Burlingame, CA) for 1 hour and then streptavidin conjugated dylight (1:33, Vector Labs, Burlingame, CA) for 1 hour at room temperature. Slides were viewed under a Olympus Fluoview FV 1000 confocal microscopy. Antibody dilutions used are shown in Table 1.

Astrocyte cell culture

Retinal astrocyte cells were isolated as previously stated (Scheef et al., 2005). Briefly, retinas from one litter of 4 week old Immortomice were dissected, rinsed in serum free DMEM, and digested with collagenase Type I in serum free DMEM.

After rinsing in 10% FBS in DMEM, they were centrifuged for 5 minutes at 400x g, filtered through a sterile 40 μm nylon mesh, centrifuged for 5 minutes at 400x g and the medium aspirated. The cells were then resuspended in 10% FBS-DMEM with Mec 13.3 coated sheep anti rat magnetic beads, and rocked for 1 hour at 4°C. The cells were separated using a Dynal magnetic tube holder. The retinal astrocytes, not bound to the magnetic beads, were collected and washed in 10%FBS-DMEM. Cells were cultured in DMEM containing EC growth supplement (Sigma-Aldrich, St. Louis, MO), 1% Pencillin/Streptomycin (Sigma-Aldrich, St. Louis, MO), 100 mM Sodium pyruvate (Gibco), 1M HEPES (Sigma-Aldrich, St. Louis, MO), 200 mM Glutamine (Gibco, Langley, OK), 100X Non-essential amino acids (Sigma-Aldrich, St. Louis, MO), 0.35% Heparin (Sigma-Aldrich, St. Louis, MO), 10% fetal bovine serum and murine recombinant at 44U/ml interferon γ (R & D systems, Minneapolis, MN). The cells were grown on Cellbind dishes (Fisher Scientific, Pittsburgh, PA) and passaged every 3-4 days using trypsin EDTA (Sigma-Aldrich, St. Louis, MO). The mouse retinal astrocyte cells, isolated from the retinas of the immortomouse, ubiquitously expressed a temperature sensitive large T antigen. Characterization by FACS and IHC revealed that these cells are positive for Pax2, GFAP as well NG2. This observation led to the conclusion that these cells are a type of oligodendrocyte astrocyte precursor cell.

Treatment of cultured cells

Treatment of astrocyte cell cultures with sodium peroxynitrite (Cayman Chemicals, Ann Arbor, MI) was performed as previously stated in (Cassina et al., 2002b). Confluent astrocyte cell cultures were washed 3 times with phosphate buffer saline (PBS) supplemented with 0.8 mM MgCl2, 1 mM CaCl2, and 5 mM glucose. They were then incubated in 1 ml of 50 mM Na2HPO4, 90 mM NaCl, 5 mM KCl, 0.8 mM MgCl2, 1 mM CaCl2, and 5 mM glucose, pH 7.4, followed by three additions of sodium peroxynitrite.at a concentration of 0.15mM The first bolus of peroxynitrite was added to one edge of the dish and the buffer was swirled for 5 seconds to allow mixing of the peroxynitrite throughout the dish. This step was repeated twice while changing the edge at which the addition was made and then incubated for 5 minutes. The buffer was then removed, replaced with the astrocyte growth media and placed in a 5% CO_2 incubator at 33°C. The cells were then processed after 24 hours or 32 hours.

Confluent astrocyte cell cultures were treated with recombinant BMP7 or BMP4 (R&D systems, Minneapolis, MN) reconstituted in 0.4% HCl-PBS. Some dishes were treated with varying concentrations of BMP7, between 20-100 ng/ml for 24 hours, while long term experiments were treated with 100 ng/ml of BMP7 for 36 hours. Further, dishes were treated with 100 ng/ml BMP4 for 24 or 36 hours.

Cells were also treated with low and high concentration glucose solutions. 5mM and 40 mM D-glucose in DMEM were initially prepared. Astrocyte cells were

allowed to grow to about 40-50% confluency. The media was then replaced with (a) 5 mM D-glucose DMEM for a low glucose treatment, or (b) 40 mM D-glucose DMEM for a high glucose treatment. The cells were then allowed to grow for 5 days following the switch in media following which they were analyzed via RT-qPCR.

Immunocytochemistry

Autoclaved coverslips were placed in sterile 6 well plates. They were covered with 100ug/ml fibronectin in PBS for 30-45 minutes, to coat the cover slips with fibronectin. Following a rinse with DMEM, the slides were covered with 200 µl of retinal astrocyte cells suspended in DMEM. The cells were allowed to adhere to the coated cover slips by placing the plates in the 5%CO_2 incubator for 2 hours. The astrocyte growth medium was added to the wells of the plate and the cells allowed to grow to 50-60% confluency before being subject to the different treatments. Following the exposure the time, the media was removed and the slides washed thrice in 1X PBS. They were fixed in 4% paraformaldehyde for 30 minutes, incubated in methanol for 10 minutes at room temperature and washed twice in 1X PBS. Antigen retrieval was performed by incubating the slides in 0.1% SDS in 0.01 M PBS for 5 minutes followed by 3 washes in 1X PBS. To reduce autofluorescence, slides were incubated with 1% sodium borohydrite in PBS for 2 minutes at room temperature, then rinsed with 1X PBS. Cells were blocked with 4% serum in 1X PBS containing 0.25% Triton X-100 at room temperature for 1 hour. The primary antibody was diluted in 0.025% TritonX-100

PBS with 2% blocking serum, and incubated with the cover slips overnight at 4°C. Following two 1X PBS washes, the cover slips were incubated with Dylight conjugated secondary antibody diluted in 1X PBS for 1 hour at room temperature, in the dark. The cover slips were washed twice in 1X PBS and incubated with 2 µg/ml Hoechst stain diluted in 1X PBS for 2 minutes. They were then washed once with 1X PBS and mounted onto slides with Aqua Polymount. Slides were viewed under Olympus Fluoview FV 1000 confocal microscopy. Antibody dilutions used are shown in Table 1.

Western blot analysis

Following treatment, retinal astrocyte cells were lysed using Radioimmunoprecipitation assay (RIPA) lysis buffer (5M NaCl, 1M Tris, 0.5M EDTA, 5%TritonX 100 at pH 8.0 with 4% protease inhibitor cocktail and 1% PMSF) for 20 minutes on ice. Cell lysates were collected, centrifuged at 140000 rpm for 15 minutes at 4°C and the total protein concentration analyzed from the supernatant using the Bicinchonic acid (BCA) protein estimation method (Thermoscientific, Rockford, IL). Fifty micrograms of the total protein mixed with the loading dye in a 1:3 ratio was then loaded and run on a 4-20% SDS polyacrylamide gel (Nalgene) at 125 volts for 1 hour. Proteins were transferred to a Polyvinylidene fluoride (PVDF) membrane (Biorad, Hercules, CA) and subjected to immunoblotting. Prior to incubation with the antibody, the membrane was blocked using a 5% milk solution in Tris Buffered Saline-Tween (TBST;

composition – 20mM Tris base, 137mM sodium chloride, 1M HCl, 0.1% Tween-20, at pH 7.6) for 1 hour. The blots were then incubated with the primary antibody diluted in TBST at 4°C overnight. The blots were washed twice with TBST and then incubated with a peroxidase conjugated secondary antibody (Thermoscientific, Rockford, IL) diluted to 1:5000 in TBST for 1 hour in the dark at room temperature. The blots were incubated with either Pierce ECL Western Blotting Substrate (Thermoscientific, Rockford, IL) or SuperSignal West Femto Chemiluminescent Substrate (Thermoscientific, Rockford, IL) and the bands visualized on x-ray films (Thermoscientific, Rockford, IL). Densitometry of the blots was performed using the Image J software (http://rsbweb.nih.gov/ij/). β Tubulin was used as a loading control. Antibody dilutions used are shown in Table 2.

Real Time-Quantitative PCR (RT-qPCR)

Total RNA was extracted from mouse retinal astrocyte cells cultures using RNeasy Mini Kit (Qiagen, Valencia, CA). Prior to cDNA synthesis, RNA samples were run on a 1% agarose gel to confirm the overall quality of the total RNA. cDNA was synthesized from 1µg of total RNA with iScript cDNA synthesis kit (Biorad, Hercules, CA) according to the manufacturer's protocol. RT-qPCR was performed using 7300 RT detection system (Applied Biosystems, Carlsbad, CA) using the Power SYBR green PCR master mix (Invitrogen, Grand Island, NY). The primer pairs used have been listed in Table 3. Total volume for each reaction was 20 µl using the diluted cDNA, corresponding to 5ng of initial total RNA and

0.4mM of each primer. The cycler conditions used were as follows: initial denaturation at 95°C for 10 minutes, 40 cycles of denaturation at 95°C for 15 seconds, annealing at 60°C for 30 seconds and extension at 72°C for 30 seconds, followed by a final extension at 72°C for 5 minutes. Efficiency of the primer sets was determined by the standard curve method, where efficiency, $E= ((10^{(-1/C_{T2} - C_{T1})}) - 1) \times 100$. A no template control and an internal control - Beta 2 microglobulin (B2M) were used for each run (Thal et al., 2008). The amplified samples were run on a 2% agarose gel to confirm amplification was of the right size. The change in the gene expression levels was done using the $2^{-\Delta\Delta C_T}$ method, where C_T is the crossing threshold value.

$\Delta C_T = C_{T\ Target\ gene} - C_{T\ B2M}$ and $\Delta\Delta C_T = \Delta C_{T\ treated} - \Delta C_{T\ control}$

Statistical Analysis

Statistical analysis of RT-qPCR data was by unpaired *t-test* between the control and treated groups. Statistical analysis of densitometry results was by students *t-test*. All analyses were performed using SPSS software (IBM) and Excel 2010 (Microsoft).

CHAPTER 3 RESULTS

Reactive retinal gliosis *in vivo*

The 2 animal models, WPK rat and $Ins2^{Akita}$ mouse, were assessed for reactivity via immunohistochemistry for the expression of GFAP, glutamine synthetase, S100-β and neurocan (Fig. 8, 9 and 10). In the $Ins2^{Akita}$ mouse model, the increase in expression of GFAP, glutamine synthetase, S100-β and neurocan was more in the diseased eye when compared to the wild type, at 6 week stage (Fig. 9). In the WPK rat model, the 3 week old rat eye sections showed a marked increase in the expression of GFAP, glutamine synthetase and S100-β (Fig. 10 E, F and H) when compared to wild type (Fig. 10 A, B and D). The neurocan levels were increased in the WPK rat but its expression was not upregulated to the same extent as the other markers (Fig. 10 C and G). The reactive gliosis apparent at the 6 week time point of the $Ins2^{Akita}$ was moderate in comparison to the more severe gliosis present in the WPK model The neurocan expression, on the other hand, was observed to be upregulated to a more intense level in the mouse model than in the rat model.

Whole retinas isolated from the eyes of 3 and 6 week $Ins2^{Akita}$ mouse were also analyzed by RT-qPCR for a panel of markers to assess reactivity (Fig. 11 A and

B). In the 3 week Ins2^{Akita}, we observe a less than 1.5 fold increase in the GFAP RNA levels. However, we do observe a fold increase in the levels of PAX2, S100 and MMP11 (Fig. 11 A). By the 6 week stage, GFAP levels do increase to about 2 fold times that of the wild type. We also observe a 2 fold increase in the levels of EGFR1. But, the levels of markers S100, MMP11 and MMP14 fall below the wild type levels with S100 and MMP14 levels falling to about half of the wild type controls (Fig. 11 B).

RNA from the whole retinas was also analyzed via RT-qPCR for the expression of some of the BMP molecules as well as some of the downstream signaling components (Fig. 12 A and B). We observed that at the 3 week stage, the RNA levels of BMP -2, -4, -6 and -7 RNA to be greater than the wild type controls. Further, at this stage, the levels of BMP -2, -4 and -6 appeared to be greater in comparison to the levels of BMP7 (Fig. 12 A). However, by the 6 week stage, levels of BMP7 RNA had gone up, while that of BMP -2, -4 and -6 had subsided. We also observed at this stage the levels of ID3 and SMAD7 to be increased, which further indicated towards an active BMP signaling mechanism (Fig. 12 B).

BMP7 expression *in vivo*

To determine if BMP7 expression was upregulated in the diseased models when compared to their respective wild types, immunohistochemistry was performed using antibody against BMP7. In both the 6 week Ins2^{Akita} mouse and the WPK rat model (Fig. 13 G and I), the expression of BMP7 was upregulated when

compared to their respective wild types (Fig. 13 A and C). In the WPK rat, the expression is restricted to the photoreceptors and in the $Ins2^{Akita}$ mouse, it is widespread. The WPK cystic rat showed a much more marked increase in the expression of BMP7 when compared to the 6 week $Ins2^{Akita}$ mouse model.

pSMAD1 expression *in vivo*

$Ins2^{Akita}$ mouse and 3 week WPK rat retinas were further assessed for pSMAD activity via immunohistochemistry to assess BMP signaling in the retina. IHC for pSMAD1 and glutamine synthetase showed an increase in labeling for pSMAD1 in the 3 week $Ins2^{Akita}$ (Fig. 14 D) retina when compared to wild type (Fig. A). Colocalization of pSMAD1 and glutamine synthetase was observed in some processes in the outer nuclear and plexiform layers (Fig. 14 C and F). The 6 week $Ins2^{Akita}$ mouse (Fig. 15 D) and 3 week WPK rat retinas (Fig. 16 D) also showed an increase in the expression of pSMAD1 when compared to the respective wild types (Fig. 15 A and 16 A, respectively). In the 6 week $Ins2^{Akita}$ and the WPK rat retinas, pSMAD1 expression was increased in the ganglion cell layer and the inner nuclear layers. pSMAD1 labeling was observed in some processes in the outer plexiform and outer nuclear layer (Fig. 14, 15 and 16).

Reactivity *in vitro* – treatment with sodium peroxynitrite and high glucose solution

In order to analyze whether BMP7 alone could initiate reactive gliosis, we turned to an *in* vitro model system using astrocytes isolated from mouse retina. To establish a reactive astrogliosis model *in vitro*, retinal astrocyte cells were treated

with sodium peroxynitrite, a strong oxidizing agent similar to superoxide ions released by neurons upon injury, to mimic injury conditions *in vitro,* as well as a high glucose solution in DMEM to mimic the hyperglycemic conditions of diabetes. Astrocytes exposed briefly to 0.15mM sodium peroxynitrite were analyzed 32 hours later for changes in expression of GFAP, GS and S100-β via immunocytochemistry (Fig. 17). In all cases the intensity of staining seemed to be higher in the sodium peroxynitrite treated cells. To quantify the change in expression of proteins, western blot analysis was performed. As was observed in the immunocytochemistry, densitometric analysis of the western blots also showed an upregulation of GFAP and GS in the sodium peroxynitrite treated cells when compared to the vehicle treated cells (Fig. 18). The treated cells were also analyzed for changes in expression of several astrocyte specific markers, extracellular matrix molecules, signaling molecules and receptors at the RNA level, via RT-qPCR (Fig. 19). An initial panel of markers used to analyze the reactivity *in vitro* consisted of about 30 markers, classified into: astrocyte specific markers, receptors and signaling molecules, chondroitin sulfate proteoglycans and matrix metalloproteinases and their tissue inhibitors. Many of the markers, including GFAP, S100, neurocan and MMPs, observed to increase following exposure to peroxynitrite, have been previously shown to be upregulated in reactive conditions (Sofroniew, 2009). Changes in the RNA levels of these markers were also analyzed following high glucose treatments. However, changes in RNA levels of the gliosis markers were not as high as in the

peroxynitrite treatment; although, an increase in the levels of astrocyte specific marker GFAP as well as some of the receptors was observed (Fig. 20).

Treatment with BMP7 induces reactivity

To determine the role of BMP7 in reactivity, the retinal astrocyte cells were treated with recombinant mouse BMP7 for 24 and 36 hours. Analysis of levels of RNA via RT-qPCR following the treatments with BMP7 revealed that at the 24 hour mark, a marker pool largely similar, but not identical, to that seen in the sodium peroxynitrite treatments were affected (Fig. 21 A). By the 36 hour time point most of the markers had reduced back to control levels, although the TIMPs and the MMPs still showed high levels of RNA expression (Fig. 21 B). Protein expression levels in the 24 hour BMP7 treatments, as analyzed by western blotting, showed a 2 fold increase in the GFAP expression levels and a 1.5 fold increase in GS levels (Fig. 22). Based on the statistical analysis of the expression levels in the sodium peroxynitrite treatment studies and the 24 and 36 hour treatment studies, a panel of 12 markers (Table 4) was built to assess reactivity in future experiments.

BMP7 has a complex relationship with the reactivity markers

To assess how expression of various markers depended on BMP signaling, the retinal astrocyte cells were treated with varying concentrations of BMP7 (20, 40, 60 and 80 ng/ml) for 24 hours and analyzed for the regulation of expression of reactivity panel markers. We observed that most of the markers did have a linear

relationship with the BMP7 concentration. Some such as GFAP2 and PAX2 showed a positive correlation with the BMP7 gradient, the matrix metalloproteinases (MMP-9 and -11) showed an inverse correlation. The chondroitin sulfate proteoglycans (phosphacan and neurocan) and receptor molecules (epidermal growth factor receptor-1 and toll like receptor-4) showed a more complex relation (Fig. 23).

Effect of treatment with BMP4

To determine if treatment with other BMPs also induced reactivity *in vitro*, mouse retinal astrocyte cells were treated with 100ng/ml of BMP4 for 24 or 36 hours. Following treatment, cells were analyzed via RT-qPCR for changes in the levels of RNA of the reactivity panel (Fig. 24 A and B). At the 24 hour time point we see about a 1.5 fold increase in the RNA levels of GFAP, EGFR1 and neurocan (Fig. 24 A). By the 36 hour time point, the RNA levels of most of the markers had returned to control levels (Fig. 24 B). Levels of MMP9 remained at about half that of the control levels in both the 24 hour and 36 hour treatments. We observed that in the BMP4 treated cells, the RNA levels of the markers were not regulated to the same extent as seen in BMP7 treatments, both the 24 and 36 hour treatments.

BMP signaling in gliosis *in vitro*

To assess BMP signaling in gliosis in vitro, cells treated with sodium peroxynitrite and high glucose DMEM were analyzed for RNA levels of the BMP molecules

and downstream signaling components previously analyzed (Fig. 25 A and B). We observed there is an increase in the levels of BMP4, BMP6 and BMP7 as well as ID1 and MSX2 in the peroxynitrite treated cells when compared to the control treatments. Both peroxynitrite and high glucose treatment conditions did increase the RNA levels of BMP4 and BMP7. Further, peroxynitrite treatment also showed increased levels of BMP6 along with a very large increase in levels of ID1. While high glucose treatments showed an increase in levels of BMP2 and ID3. This suggests that BMP signaling is active in reactive gliosis in vitro and may play a role in regulation of the RNA levels of various markers. Further, analysis of protein from the peroxynitrite treated cells and for phospho SMAD1, 5, 8 via western blotting and pSMAD1 via immunocytochemistry showed an increase in the levels of the protein (Fig. 26 and 27).

CHAPTER 4 DISCUSSION

Summary of results

To initially characterize reactivity *in vivo*, the retinal tissue sections of 2 models, the Ins2^{Akita} mouse and the WPK rat were analyzed via IHC for gliosis markers and compared to their respective wild types. The 3 week Ins2^{Akita} did not show an increase in labeling for the markers analyzed. The 6 week Ins2^{Akita} mouse and the 3 week WPK rat did show an increase in expression of GFAP, S100-β and glutamine synthetase. Further, the 6 week Ins2^{Akita} mouse also showed an increase in expression of the inhibitory CSPG – neurocan. RT-qPCR analysis of RNA from whole retinas of the 3 and 6 week Ins2^{Akita} showed results consistent with the IHC observations. RT-qPCR for different BMP molecules and its downstream components showed that RNA levels of BMP-2, -4, -6 and -7 to be greater than the wild type controls. However, in the 6 week Ins2^{Akita}, BMP7 showed over a 3 fold increase when compared to about a 1.5 fold increase in the 3 week Ins2^{Akita}, over the respective wild type controls. When analyzed for BMP7 expression via IHC, the 6 week Ins2^{Akita} mouse and WPK rat retinal tissue sections showed more labeling in the diseased/mutant retinas which were previously shown to have reactive gliosis. To determine BMP signaling in the diseased/mutant retinas, the 6 week Ins2^{Akita} mouse and the 3 week WPK rat

retinal tissues were analyzed for pSMAD1 expression. The $Ins2^{Akita}$ and 3 week WPK rat retina did show an increase in pSMAD1 labeling.

To assess reactivity further in retinal astrocytes, astrocytes were first isolated from the retinas of 4-6 week old immortomouse. The cells which could be maintained in culture were subjected to different treatment conditions. As a first step, cells were treated with sodium peroxynitrite and analyzed via RT-qPCR, ICC and western blotting. Treatment with sodium peroxynitrite did induce a reactive astrocyte state in the astrocytes which was confirmed by the increase in RNA levels of various markers via RT-qPCR as well as an increase in GFAP via western blotting. The cells were exposed to a 5 day glucose DMEM media to mimic the hyperglycemic conditions of $Ins2^{Akita}$. RT-qPCR analysis of the RNA from the treated cells did show an increase in the expression of GFAP along with some of the other gliosis markers. The cells were also treated with BMP7 and BMP4 to determine if they did play a role in making astrocytes reactive. The cells were treated with BMP7 and BMP4 for 24 and 36 hours. With BMP7 treatments, we did observe reactivity in the astrocyte cells at the 24 hour time point, confirmed by RT-qPCR as well as western blotting for GFAP. By 36 hours, most of the gliosis markers had normalized. The BMP4 treatments did not induce changes in the RNA levels of the gliosis markers to an extent similar to the BMP7 treatments in both the 24 hour and 36 hour treatments. The cells were then subject to treatments with different concentrations of BMP7 to analyze the changes in levels of RNA of the gliosis markers. We observed that a group of the

markers did show a direct correlation with changes in BMP7 concentration while others showed a mixed correlation with the change in growth factor concentration.

The peroxynitrite and glucose treated cells were also analyzed via RT-qPCR for the changes in the levels of various BMP molecules, the SMAD signaling components and a few downstream targets. We did observe an increase in the levels of RNA of BMP7 in the peroxynitrite treated cells and not in the glucose treated cells. Further, we did observe an increase in pSMAD levels in the peroxynitrite treated cells which were analyzed via western blotting and ICC. The increase in the levels of pSMAD was similar to that seen in the BMP7 treated cells, indicating an active BMP mechanism in these reactive cells.

$Ins2^{Akita}$ mouse and WPK rats as models for reactive gliosis in the retina and BMP expression

The $Ins2^{Akita}$ mice have a point mutation replacing a cysteine with a tyrosine residue at the seventh amino acid residue of the A chain of the insulin 2 gene product, leading to a conformation change in the protein by blocking the formation of an essential disulfide bond. The $Ins2^{Akita}$ mouse model has been previously used as a model to study abnormalities in the retina brought on by diabetes (Barber et al., 2005). In the retina, loss of amacrine cells have been reported in these animals (Gastinger et al., 2006). The increased glucose in

these animals, which has previously been shown to make astrocytes *in vitro* reactive (Wang et al., 2012), coupled with a loss of neurons in the retina makes this model a good option to study reactive gliosis.

The WPK rat model is used to study the Meckel-Gruber syndrome (MKS). MKS is an “autosomal, recessive, lethal, malformation syndrome characterized by renal cystic dysplasia, CNS malformations and polydactyly”. Mutation in the gene MKS3 (which encodes for mecklin protein) has been implicated in the model system (Smith et al., 2006). Due to this mutation, functional defects have been reported in the connecting cilium in the eye lead to a lack of formation of outer segments and this leads to defective eyes in this model (Collin et al., 2012). The rationale behind choosing this model to study reactive gliosis is the loss of photoreceptor outer segments in the retinas of this model which may serve as a stimulus in making astrocytes reactive.

To determine reactivity in the 2 animal models, retinal tissue sections from the eyes of the animals were analyzed via immunohistochemistry for some of the markers previously shown to be regulated in gliosis. Of the 2 models used in the study, the WPK appears to be a more severe model of gliosis than the $Ins2^{Akita}$ mouse model, as seen by IHC analysis for markers GFAP, GS, S100-β and neurocan. In both the WPK and the 6 week $Ins2^{Akita}$ model, there seemed to be an upregulation of GS and GFAP. Neurocan seemed to be upregulated more in the $Ins2^{Akita}$ mouse model than in the WPK rat model. The finding that there is

less reactive gliosis and yet more glial scar components such as neurocan is intriguing and is consistent with the idea that reactive gliosis can play beneficial roles in injury and disease (Myer et al., 2006, Sofroniew, 2009). The 3 week stage of the mouse did not show change in expression of the markers analyzed in comparison to the wild type. In the $Ins2^{Akita}$ mouse, at the 3 week there is little or no retinal complications seen due to diabetes in the mouse (Barber et al., 2005). Thus, the retina, as analyzed by IHC, does not appear to have largely different expression patterns than the wild type at this stage. Consistent with this idea, RT-qPCR analysis of RNA from whole retinas of 3 and 6 week mouse model systems did show the regulation of more markers at the 6 week stage than the 3 week stage, correlating with the IHC results.

IHC and RT-qPCR did show the 6 week $Ins2^{Akita}$ and the 3 week WPK rat retinas to have reactive astrocytes. Studies previously done using spinal cord injury models to understand reactive gliosis, did show an increase in BMPs in the site of injury and to play a role in the specification of astrocyte/oligodendrocyte precursors (Setoguchi et al., 2004, Xiao et al., 2010). RT-qPCR analysis of RNA from whole retinas of the 3 and 6 week $Ins2^{Akita}$ mouse model showed an increase in the levels of RNA of BMP7 when comparing the 3 and 6 week $Ins2^{Akita}$ mouse. As a first step to identify BMP signaling in reactive gliosis, retinal tissue sections of the $Ins2^{Akita}$ mouse and the 3 week WPK rat were analyzed via IHC for BMP7, which has been previously reported to be increased following injury (Setoguchi et al., 2001, Sahni et al., 2010). IHC for BMP7 revealed

increased expression in the WPK and the 6 week $Ins2^{Akita}$ mouse model. In the rat, the expression of BMP7 was seen primarily in the outer layers of the retina and this can be attributed to an increase in reactive oxygen species that result from a loss of functional photoreceptors. In comparison to the WPK model, the $Ins2^{Akita}$ mouse model, the BMP7 protein was localized to the inner layers of the retina. Western blotting analysis need to be performed, to quantitate the levels of BMP7. We further investigated the increase in BMP signaling by analyzing the expression of phospho-SMAD (pSMAD1). pSMAD is the activated form of the receptor linked SMAD1 molecule. The canonical BMP signaling pathway proceeds via activation of the SMAD 1, 5 and 8 molecules (Nohe et al., 2004). The retinas of the $Ins2^{Akita}$ and the 3 week WPK rat did show an increase in labeling for pSMAD1 when compared to their respective wild type. This increase in the RNA levels as well as in the protein levels, analyzed by RT-qPCR and IHC, respectively, of BMP7, coupled with the signs of reactivity confirmed by RT-qPCR and IHC in the animal models are indicative for a role of BMP7 in regulation gliosis in these model systems.

In vitro reactivity model using sodium peroxynitrite and high glucose DMEM

The 2 animal models previously described, help setup an *in vivo* model system to understand gliosis. However, using an *in vitro* model system would be more advantageous as it is more amenable to different manipulations. The first step in *in vitro* analysis was to mimic reactivity. Peroxynitrite is a toxic metabolite of nitric oxide and a strong oxidizing agent which has previously been shown to play a

role in oxidative stress and mediating motor neuron apoptosis. Peroxynitrite induces the inducible nitric oxide synthase in the astrocytes and this leads to an increase in production of nitric oxide which leads to a neurotoxic effect (Cassina et al., 2002a). Peroxynitrite leads to long term inhibition of gap junction communications between astrocytes and neurons as well as inhibition of axonal conduction and the mitochondrial respiratory chain, thereby increasing the neurotoxic effects on neurons (Redford et al., 1997, Stewart et al., 2000). Previous studies have shown that spinal cord astrocytes exposed to peroxynitrite underwent morphological transformations which induced motor neuron apoptosis. In this study we have shown that treatment of retinal astrocyte cell cultures with sodium peroxynitrite induces changes in expression of several markers including GFAP. Western blot analysis did show the increase in GFAP protein levels to be about 1.5 fold that of the control cells. Immunocytochemistry has revealed that there is a change in expression of other astrocytic markers such as glutamine synthetase (GS) and S100-β, as well the BMP pathway signaling molecule – phospho-SMAD1 (pSMAD1). These findings are in agreement with previous reports showing that exposure of astrocytes to peroxynitrite induces reactive phenotypic changes. Cells treated with peroxynitrite were analyzed via RT-qPCR for the RNA levels of various markers including astrocyte specific markers, signaling molecules and receptors as well as extra cellular matrix molecules such as the inhibitory CSPGs, MMPs and TIMPs. We observed that peroxynitrite treated cells did have increased RNA levels of astrocytic markers such as GFAP, PAX2 and S100, along with an

increase in the levels of inhibitory CSPGs and other extracellular molecules such as the MMPs and TIMPs. These results coupled with the immunocytochemistry analysis and an increase in GFAP protein levels shown by the western blotting show that sodium peroxynitrite treatments are a viable method to make astrocyte cells reactive *in vitro*.

The peroxynitrite treatment was analogous to an *in vivo* injury model system. To mimic the hyperglycemic conditions of the diabetes in the $Ins2^{Akita}$, cells in culture were exposed to 40mM glucose in DMEM for 5 days, following which the cells were processed for RNA and analyzed via RT-qPCR for the levels of various gliosis markers previously used. The RT-qPCR data showed an increase in GFAP as well as EGFR1. The changes in the levels of RNA in the glucose treatment were not as severe as the peroxynitrite treatment conditions, and showed to be similar to the changes in levels of RNA in the 6 week $Ins2^{Akita}$ mouse, suggesting that this is an apt model to study gliosis occurring due to hyperglycemia in diabetes.

BMP7 plays a role in making astrocytes reactive

The BMPs belong to the TGF-β superfamily of proteins and are involved in a wide range of functions all throughout development. One of the functions of the BMPs is the determination of glial fate in neuroepithelial precursor cells (Mabie et al., 1997, Yanagisawa et al., 2001, He and Sun, 2007). One important function of the astrocytes is reactive gliosis, which is a response in the astrocytes in

response to injury of nearby neurons (Sofroniew and Vinters, 2010). Previous studies have shown that BMPs (BMP -4 and -7) are upregulated at the site of injury (Setoguchi et al., 2001, Fuller et al., 2007). The BMPs are initially released by the injured neurons which can then interact with astrocytes, and induce the astrocytes as well to release the BMPs. These studies have shown a role for the BMPs in gliosis using the spinal cord injury model. In this study we aim to evaluate the role of BMPs in gliosis in the eye. *In vitro* studies were performed using the mouse retinal astrocyte cells previously isolated. They were initially subject to a treatment with 100ng/ml of BMP7. Initial analysis by western blot for levels of GFAP did show a 2 fold increase in protein levels indicating that BMP7 did have the potential to make cells reactive. RNA from cells treated with 100ng/ml BMP7 for 24 and 36 hours was then analyzed for changes in RNA levels of different gliosis markers. The 2 time points chosen represent an early and a late response time in the astrocytes following BMP7 treatments. We observed that at the 24 hour stage, the RNA levels of a larger set of markers including GFAP, PAX2, SMADs, as well as extra cellular molecules including the inhibitory CSPGs, MMPs and TIMPs were regulated. By the 36 hour stage, most of the markers had normalized to control levels except for some of the CSPGs, TIMPS and MMPs. By the 36 hour point, the BMP signaling has most likely subsided and this may be the reason for the normalization of the RNA levels of the different markers. One treatment with BMP7 may be analogous to a mild injury of the CNS which is why we see the normalization of markers by the 36 hour stage.

To further evaluate the role of BMP7 in gliosis, mouse retinal astrocyte cells were treated with varying concentrations of BMP7 and we observed the RNA levels a panel of markers which have been found to be regulated in gliosis. Most of the markers from the panel, showed a direct correlation between the levels of RNA and the concentration of BMP7. A few markers, including the inhibitory CSPGs, neurocan and phosphacan, as well as the receptors EGFR1 and TLR4 showed a more complex relation with BMP7 dosage. Increase in levels of EGFR1 following BMP7 treatment indicated towards activation of the EGFR pathway. This evidence, along with the non linear correlation between BMP treatments and RNA levels of markers suggest crosstalk between the BMP pathway and other pathways.

The BMPs can mediate signaling through a canonical – SMAD dependent pathway or the non canonical SMAD independent pathway (Nohe et al., 2004). Thus, BMPs can regulate signaling through either the SMADs or other molecules such as TAK or TAB. Activation of the later molecules may lead to activation of other signaling pathways such as NF-κB, p38 and JNK (Nohe et al., 2004, Sieber et al., 2009). Therefore, the effects seen in the RNA levels of the different gliosis markers may suggest activation of other pathways along with the BMP pathway. These pathways may either be simultaneously activated along with the BMP pathway or be regulated by the SMAD independent (TAK – TAB pathway) part of the BMP pathway. This increase in EGF receptor might indicate towards

activation of the EGF pathway, which could also regulate changes observed in gliosis (Ridet et al., 1997, Sofroniew, 2009).

Effect of other BMP molecules

As mentioned previously, BMP molecules have been shown to be upregulated at the site of nerve injury. We have looked at the role of BMP7 in gliosis using the mouse retinal astrocyte cells. BMP4 is another molecule which has been found to be upregulated at the site of the injury (Fuller et al., 2007). We determined the effect of BMP4 on mouse retinal astrocyte cells, to analyze if a reactive state similar to that of BMP7 treatments was observed. RT-qPCR analysis was performed to analyze RNA levels for reactivity markers in 100ng/ml BMP4 treated cells. Similar to the BMP7 treatments, 2 time points were chosen – 24 and 36 hour, which represented a short and long term exposure period. Apart from MMP9, which showed a significant decrease in RNA levels, the reactivity markers in the BMP4 treated cells were not altered to a significant extent.

The BMPs regulate activity by binding to 2 extracellular receptors: the type I (5 known types) and type II receptors (3 known types). The BMPs bind to the type II receptor which then leads to dimerization of the receptor with a type I receptor (Miyazono et al., 2010). The dynamics of the receptor dimerization and the downstream components activated by each complex is still unclear. Thus, treatment of astrocytes by BMP4 may activate a different set of downstream signaling components when compared with the BMP7 molecule, which may

account for the differences in the RNA levels seen in the treated retinal astrocyte cells.

BMP signaling in gliosis

Sodium peroxyitrite has been showed to make astrocyte cells in culture reactive. To analyze the RNA levels of different BMP molecules following injury, cells treated with sodium peroxynitrite were analyzed via RT-qPCR. We observed an increase in the levels of BMP4, BMP6 and BMP7 as well as the downstream targets – ID1 and MSX2 in the peroxynitrite treated cells when compared to the control treatments. Analysis of RNA levels in the $Ins2^{Akita}$ mouse model showed an increase in the levels of BMP7 at the 6 week stage, along with an increase of downstream molecules SMAD8 and MSX2. Analysis of the 3 week stage shows that the levels of BMP – 4 and 6 to be higher than BMP7. This increase in BMP7 RNA levels when comparing the 3 week to the 6 week stage coupled with the RT-qPCR and IHC data which shows gliosis at the 6 week stage, suggest there is increased BMP signaling in gliosis in the diseased state. The *in vitro* results further provide evidence that BMP signaling is active in reactive gliosis in injury conditions and may play a role in regulation of the RNA levels of various markers. Analysis of protein from the treated cells for phospho SMAD1, 5, 8 via western blotting and immunocytochemistry does show an increase in the levels of the protein. Phsospho SMAD is the activated form of the SMAD signaling molecule and its increased levels indicates towards an activation of the BMP pathway. Studies have recently implicated reactive astrocytes to play a role in

inflammation following injury (reviewed in Sofroniew and Vinters, 2010). The BMP pathway has been shown to elicit an inflammatory response by activating the NF – κB pathway via the non-canonical BMP-MAPK pathway (reviewed in Nohe et al., 2004, Bragdon et al., 2011, Hayden and Ghosh, 2012). We observe here an increase in BMP signaling as well as concomitant increase in the toll like receptor (TLR-4), suggesting that this may be a possible mechanism leading to the inflammatory response. We have thus, observed an increase in RNA and protein levels of BMP7 and pSMAD in reactive gliosis. Further, differential regulation of different markers of gliosis under different conditions and due to exposure to BMP7 suggests activation of both the SMAD dependent and independent pathways, and an active role for BMP signaling in reactive gliosis.

Future Directions

To further evaluate BMP signaling in gliosis, we propose the following experiments –

- Effect of BMP inhibitor LDN-193189, which specifically blocks the Alk2 receptor (which is the preferred receptor for BMP7 mediated signaling) on the RNA levels as well as protein expression levels of various markers for gliosis.
- Proliferation assays following treatment with BMP7 and/or its inhibitor to determine the effects of BMP signaling in the proliferative changes during gliosis.

- Studying the effects of BMP signaling and its inhibition *in vivo*. Determining if reactive gliosis is induced in normal mice retina following intra vitreal injection of BMP7 or if the gliosis condition attenuates following intra vitreal injection of LDN-193189 in Ins2Akita mouse will further gliosis mediated via the BMP7-Alk2 receptor coupled pathway.

Conclusion

We have shown here that BMP7 plays a role in reactive gliosis in retinal astrocytes. Further, we have shown here that BMP signaling plays a role in gliosis following both injury and disease. By building a panel of markers to assess reactivity via RT-qPCR, we have devised a tool which could be used for easy and quick evaluation of reactivity in astrocytes, analyzing different aspects of gliosis. BMP signaling, through the SMAD dependent or the SMAD independent mechanisms or a combination of both seem to be involved in gliosis. The role of BMPs in gliosis seems to be far from straightforward. Gliosis in the retina following injury or in disease may involve additional pathways being simultaneously activated or downstream of the BMP signaling mechanism.

In conclusion, this project has helped determine the role of BMP7 in gliosis and also revealed a more complex involvement of the BMP pathway in gliosis in the retina.

REFERENCES

REFERENCES

1. Abbott NJ, Ronnback L, Hansson E (2006) Astrocyte-endothelial interactions at the blood-brain barrier. Nature Reviews Neuroscience 7:41-53.
2. Adler R, Belecky-Adams TL (2002) The role of bone morphogenetic proteins in the differentiation of the ventral optic cup. Development 129:3161-3171.
3. Allen NJ, Barres BA (2005) Signaling between glia and neurons: focus on synaptic plasticity. Curr Opin Neurobiol 15:542-548.
4. Baker JC, Harland RM (1997) From receptor to nucleus: the Smad pathway. Curr Opin Genet Dev 7:467-473.
5. Barber AJ, Antonetti DA, Kern TS, Reiter CEN, Soans RS, Krady JK, Levison SW, Gardner TW, Bronson SK (2005) The Ins2(Akita) mouse as a model of early retinal complications in diabetes. Invest Ophth Vis Sci 46:2210-2218.
6. Barres BA (2008) The Mystery and Magic of Glia: A Perspective on Their Roles in Health and Disease. Neuron 60:430-440.
7. Belecky-Adams T, Adler R (2001) Developmental expression patterns of bone morphogenetic proteins, receptors, and binding proteins in the chick retina. J Comp Neurol 430:562-572.
8. Bond AM, Bhalala OG, Kessler JA (2012) The dynamic role of bone morphogenetic proteins in neural stem cell fate and maturation. Developmental neurobiology 72:1068-1084.
9. Bragdon B, Moseychuk O, Saldanha S, King D, Julian J, Nohe A (2011) Bone Morphogenetic Proteins: A critical review. Cell Signal 23:609-620.
10. Brambilla R, Bracchi-Ricard V, Hu WH, Frydel B, Bramwell A, Karmally S, Green EJ, Bethea JR (2005) Inhibition of astroglial nuclear factor kappa B reduces inflammation and improves functional recovery after spinal cord injury. J Exp Med 202:145-156.
11. Bringmann A, Pannicke T, Biedermann B, Francke M, Iandiev I, Grosche J, Wiedemann P, Albrecht J, Reichenbach A (2009) Role of retinal glial cells in neurotransmitter uptake and metabolism. Neurochemistry international 54:143-160.
12. Bringmann A, Pannicke T, Grosche J, Francke M, Wiedemann P, Skatchkov SN, Osborne NN, Reichenbach A (2006) Muller cells in the healthy and diseased retina. Progress in retinal and eye research 25:397-424.

13. Bush TG, Puvanachandra N, Horner CH, Polito A, Ostenfeld T, Svendsen CN, Mucke L, Johnson MH, Sofroniew MV (1999) Leukocyte infiltration, neuronal degeneration, and neurite outgrowth after ablation of scar-forming, reactive astrocytes in adult transgenic mice. Neuron 23:297-308.
14. Cassina P, Peluffo H, Pehar M, Martinez-Palma L, Ressia A, Beckman JS, Estevez AG, Barbeito L (2002a) Peroxynitrite triggers a phenotypic transformation in spinal cord astrocytes that induces motor neuron apoptosis. Journal of neuroscience research 67:21-29.
15. Cassina P, Peluffo H, Pehar M, Martinez-Palma L, Ressia A, Beckman JS, Estevez AG, Barbeito L (2002b) Peroxynitrite triggers a phenotypic transformation in spinal cord astrocytes that induces motor neuron apoptosis. Journal of neuroscience research 67:21-29.
16. Cheng H, Nair G, Walker TA, Kim MK, Pardue MT, Thule PM, Olson DE, Duong TQ (2006) Structural and functional MRI reveals multiple retinal layers. Proceedings of the National Academy of Sciences of the United States of America 103:17525-17530.
17. Chu Y, Hughes S, Chan-Ling TL (2001) Differentiation and migration of astrocyte precursor cells (APCs) and astrocytes in human fetal retina: relevance to optic nerve coloboma. Faseb J 15:2013-+.
18. Codeluppi S, Svensson CI, Hefferan MP, Valencia F, Silldorff MD, Oshiro M, Marsala M, Pasquale EB (2009) The Rheb-mTOR Pathway Is Upregulated in Reactive Astrocytes of the Injured Spinal Cord. J Neurosci 29:1093-1104.
19. Collin GB, Won J, Hicks WL, Cook SA, Nishina PM, Naggert JK (2012) Meckelin Is Necessary for Photoreceptor Intraciliary Transport and Outer Segment Morphogenesis. Invest Ophth Vis Sci 53:967-974.
20. Conidi A, Cazzola S, Beets K, Coddens K, Collart C, Cornelis F, Cox L, Joke D, Dobreva MP, Dries R, Esguerra C, Francis A, Ibrahimi A, Kroes R, Lesage F, Maas E, Moya I, Pereira PNG, Stappers E, Stryjewska A, van den Berghe V, Vermeire L, Verstappen G, Seuntjens E, Umans L, Zwijsen A, Huylebroeck D (2011) Few Smad proteins and many Smad-interacting proteins yield multiple functions and action modes in TGF beta/BMP signaling in vivo. Cytokine Growth F R 22:287-300.
21. Crocker SJ, Milner R, Pham-Mitchell N, Campbell IL (2006) Cell and agonist-specific regulation of genes for matrix metalloproteinases and their tissue inhibitors by primary glial cells. Journal of neurochemistry 98:812-823.
22. Dakubo GD, Beug ST, Mazerolle CJ, Thurig S, Wang YP, Wallace VA (2008) Control of glial precursor cell development in the mouse optic nerve by sonic hedgehog from retinal ganglion cells. Brain research 1228:27-42.
23. Derynck R, Zhang YE (2003) Smad-dependent and Smad-independent pathways in TGF-beta family signalling. Nature 425:577-584.

24. Dubois-Dauphin M, Poitry-Yamate C, De Bilbao F, Julliard AK, Jourdan F, Donati G (2000) Early postnatal Muller cell death leads to retinal but not optic nerve degeneration in NSE-HU-BCL-2 transgenic mice. Neuroscience 95:9-21.
25. Dudley AT, Lyons KM, Robertson EJ (1995) A Requirement for Bone Morphogenetic Protein-7 during Development of the Mammalian Kidney and Eye. Genes & development 9:2795-2807.
26. Eddleston M, Mucke L (1993) Molecular Profile of Reactive Astrocytes - Implications for Their Role in Neurologic Disease. Neuroscience 54:15-36.
27. Enzmann GU, Benton RL, Woock JP, Howard RM, Tsoulfas P, Whittemore SR (2005) Consequences of noggin expression by neural stem, glial, and neuronal precursor cells engrafted into the injured spinal cord. Exp Neurol 195:293-304.
28. Faulkner JR, Herrmann JE, Woo MJ, Tansey KE, Doan NB, Sofroniew MV (2004) Reactive astrocytes protect tissue and preserve function after spinal cord injury. J Neurosci 24:2143-2155.
29. Fuhrmann S (2010) Eye Morphogenesis and Patterning of the Optic Vesicle. Curr Top Dev Biol 93:61-84.
30. Fuller ML, DeChant AK, Rothstein B, Caprariello A, Wang R, Hall AK, Miller RH (2007) Bone morphogenetic proteins promote gliosis in demyelinating spinal cord lesions. Ann Neurol 62:288-300.
31. Furuta Y (2000) Bmp4 is essential for lens induction in the mouse embryo. Developmental biology 222:248-248.
32. Gastinger MJ, Singh RSJ, Barber AJ (2006) Loss of cholinergic and dopaminergic amacrine cells in streptozotocin-diabetic rat and Ins2(Akita)-diabetic mouse retinas. Invest Ophth Vis Sci 47:3143-3150.
33. Ghosh-Choudhury N, Abboud SL, Nishimura R, Celeste A, Mahimainathan L, Choudhury GG (2002) Requirement of BMP-2-induced phosphatidylinositol 3-kinase and Akt serine/threonine kinase in osteoblast differentiation and Smad-dependent BMP-2 gene transcription. Journal of Biological Chemistry 277:33361-33368.
34. Gordon GRJ, Mulligan SJ, MacVicar BA (2007) Astrocyte control of the cerebrovasculature. Glia 55:1214-1221.
35. Greene NDE, Copp AJ (2009) Development of the vertebrate central nervous system: formation of the neural tube. Prenatal Diag 29:303-311.
36. Gris P, Tighe A, Levin D, Sharma R, Brown A (2007) Transcriptional regulation of scar gene expression in primary astrocytes. Glia 55:1145-1155.
37. Hampton DW, Asher RA, Kondo T, Steeves JD, Ramer MS, Fawcett JW (2007) A potential role for bone morphogenetic protein signalling in glial cell fate determination following adult central nervous system injury in vivo. The European journal of neuroscience 26:3024-3035.
38. Harrington MJ, Hong E, Brewster R (2009) Comparative Analysis of Neurulation: First Impressions Do Not Count. Mol Reprod Dev 76:954-965.

39. Hayden MS, Ghosh S (2012) NF-kappa B, the first quarter-century: remarkable progress and outstanding questions. Genes & development 26:203-234.
40. He F, Sun YE (2007) Glial cells more than support cells? Int J Biochem Cell B 39:661-665.
41. Hernandez MR, Miao HX, Lukas T (2008) Astrocytes in glaucomatous optic neuropathy. Prog Brain Res 173:353-373.
42. Herpin A, Cunningham C (2007) Cross-talk between the bone morphogenetic protein pathway and other major signaling pathways results in tightly regulated cell-specific outcomes. Febs J 274:2977-2985.
43. Herrmann JE, Imura T, Song BB, Qi JW, Ao Y, Nguyen TK, Korsak RA, Takeda K, Akira S, Sofroniew MV (2008) STAT3 is a critical regulator of astrogliosis and scar formation after spinal cord injury. J Neurosci 28:7231-7243.
44. Hertz L, Zielke HR (2004) Astrocytic control of glutamatergic activity: astrocytes as stars of the show. Trends in neurosciences 27:735-743.
45. Hogan BL (1996) Bone morphogenetic proteins: multifunctional regulators of vertebrate development. Genes & development 10:1580-1594.
46. Huxlin KR, Sefton AJ, Furby JH (1992) The Origin and Development of Retinal Astrocytes in the Mouse. Journal of neurocytology 21:530-544.
47. Jadhav AP, Roesch K, Cepko CL (2009) Development and neurogenic potential of Muller glial cells in the vertebrate retina. Progress in retinal and eye research 28:249-262.
48. Jena N, MartinSeisdedos C, McCue P, Croce CM (1997) BMP7 null mutation in mice: Developmental defects in skeleton, kidney, and eye. Experimental cell research 230:28-37.
49. Kuchler-Bopp S, Delaunoy JP, Artault JC, Zaepfel M, Dietrich JB (1999) Astrocytes induce several blood-brain barrier properties in non-neural endothelial cells. Neuroreport 10:1347-1353.
50. Laabs T, Carulli D, Geller HM, Fawcett JW (2005) Chondroitin sulfate proteoglycans in neural development and regeneration. Curr Opin Neurobiol 15:116-120.
51. Lamb TD, Collin SP, Pugh EN, Jr. (2007) Evolution of the vertebrate eye: opsins, photoreceptors, retina and eye cup. Nature reviews Neuroscience 8:960-976.
52. Levin LA (1999) Direct and indirect approaches to neuroprotective therapy of glaucomatous optic neuropathy. Survey of ophthalmology 43 Suppl 1:S98-101.
53. Liu B, Neufeld AH (2004) Activation of epidermal growth factor receptor causes astrocytes to form cribriform structures. Glia 46:153-168.
54. Luo G, Hofmann C, Bronckers ALJJ, Sohocki M, Bradley A, Karsenty G (1995) Bmp-7 Is an Inducer of Nephrogenesis, and Is Also Required for Eye Development and Skeletal Patterning. Genes & development 9:2808-2820.

55. Mabie PC, Mehler MF, Marmur R, Papavasiliou A, Song Q, Kessler JA (1997) Bone morphogenetic proteins induce astroglial differentiation of oligodendroglial-astroglial progenitor cells. J Neurosci 17:4112-4120.
56. Matsuura I, Taniguchi J, Hata K, Saeki N, Yamashita T (2008a) BMP inhibition enhances axonal growth and functional recovery after spinal cord injury. Journal of neurochemistry 105:1471-1479.
57. Matsuura I, Taniguchi J, Hata K, Saeki N, Yamashita T (2008b) BMP inhibition enhances axonal growth and functional recovery after spinal cord injury. J Neurochem 105:1471-1479.
58. Mehler MF, Mabie PC, Zhang DM, Kessler JA (1997) Bone morphogenetic proteins in the nervous system. Trends in neurosciences 20:309-317.
59. Mehler MF, Mabie PC, Zhu G, Gokhan S, Kessler JA (2000) Developmental changes in progenitor cell responsiveness to bone morphogenetic proteins differentially modulate progressive CNS lineage fate. Developmental neuroscience 22:74-85.
60. Miyazono K, Kamiya Y, Morikawa M (2010) Bone morphogenetic protein receptors and signal transduction. J Biochem 147:35-51.
61. Morcillo J, Martinez-Morales JR, Trousse F, Fermin Y, Sowden JC, Bovolenta P (2006) Proper patterning of the optic fissure requires the sequential activity of BMP7 and SHH. Development 133:3179-3190.
62. Myer DJ, Gurkoff GG, Lee SM, Hovda DA, Sofroniew MV (2006) Essential protective roles of reactive astrocytes in traumatic brain injury. Brain : a journal of neurology 129:2761-2772.
63. Nagase H, Visse R, Murphy G (2006) Structure and function of matrix metalloproteinases and TIMPs. Cardiovasc Res 69:562-573.
64. Nakayama T, Gardner H, Berg LK, Christian JL (1998) Smad6 functions as an intracellular antagonist of some TGF-beta family members during Xenopus embryogenesis. Genes Cells 3:387-394.
65. Nakazawa T, Matsubara A, Noda K, Hisatomi T, She H, Skondra D, Miyahara S, Sobrin L, Thomas KL, Chen DF, Grosskreutz CL, Hafezi-Moghadam A, Miller JW (2006) Characterization of cytokine responses to retinal detachment in rats. Molecular vision 12:867-878.
66. Neufeld AH, Sawada A, Becker B (1999) Inhibition of nitric-oxide synthase 2 by aminoguanidine provides neuroprotection of retinal ganglion cells in a rat model of chronic glaucoma. Proceedings of the National Academy of Sciences of the United States of America 96:9944-9948.
67. Nohe A, Keating E, Knaus P, Petersen NO (2004) Signal transduction of bone morphogenetic protein receptors. Cell Signal 16:291-299.
68. Pekny M, Johansson CB, Eliasson C, Stakeberg J, Wallen A, Perlmann T, Lendahl U, Betsholtz C, Berthold CH, Frisen J (1999) Abnormal reaction to central nervous system injury in mice lacking glial fibrillary acidic protein and vimentin. Journal of Cell Biology 145:503-514.
69. Pfrieger FW, Barres BA (1997) Synaptic efficacy enhanced by glial cells in vitro. Science 277:1684-1687.

70. Pizzi MA, Crowe MJ (2007) Matrix metalloproteinases and proteoglycans in axonal regeneration. Exp Neurol 204:496-511.
71. Qin WM, Zhao BT, Shi Y, Yao CG, Jin L, Jin YX (2009) BMPRII is a direct target of miR-21. Acta Bioch Bioph Sin 41:618-623.
72. Rajan P, Panchision DM, Newell LE, McKay RDG (2003) BMPs signal alternately through a SMAD or FRAP-STAT pathway to regulate fate choice in CNS stem cells. Journal of Cell Biology 161:911-921.
73. Redford EJ, Kapoor R, Smith KJ (1997) Nitric oxide donors reversibly block axonal conduction: demyelinated axons are especially susceptible. Brain : a journal of neurology 120:2149-2157.
74. Renault-Mihara F, Okada S, Shibata S, Nakamura M, Toyama Y, Okano H (2008) Spinal cord injury: emerging beneficial role of reactive astrocytes' migration. The international journal of biochemistry & cell biology 40:1649-1653.
75. Rhodes KE, Fawcett JW (2004) Chondroitin sulphate proteoglycans: preventing plasticity or protecting the CNS? J Anat 204:33-48.
76. Ridet JL, Malhotra SK, Privat A, Gage FH (1997) Reactive astrocytes: cellular and molecular cues to biological function. Trends in neurosciences 20:570-577.
77. Rompani SB, Cepko CL (2010) A Common Progenitor for Retinal Astrocytes and Oligodendrocytes. J Neurosci 30:4970-4980.
78. Rosenberg GA (2002) Matrix metalloproteinases in neuroinflammation. Glia 39:279-291.
79. Rowitch DH, Kriegstein AR (2010) Developmental genetics of vertebrate glial-cell specification. Nature 468:214-222.
80. Sahni V, Mukhopadhyay A, Tysseling V, Hebert A, Birch D, McGuire TL, Stupp SI, Kessler JA (2010) BMPR1a and BMPR1b signaling exert opposing effects on gliosis after spinal cord injury. J Neurosci 30:1839-1855.
81. Scheef E, Wang S, Sorenson CM, Sheibani N (2005) Isolation and characterization of murine retinal astrocytes. Molecular vision 11:613-624.
82. Setoguchi T, Nakashima K, Takizawa T, Yanagisawa M, Ochiai W, Okabe M, Yone K, Komiya S, Taga T (2004) Treatment of spinal cord injury by transplantation of fetal neural precursor cells engineered to express BMP inhibitor. Exp Neurol 189:33-44.
83. Setoguchi T, Yone K, Matsuoka E, Takenouchi H, Nakashima K, Sakou T, Komiya S, Izumo S (2001) Traumatic injury-induced BMP7 expression in the adult rat spinal cord. Brain research 921:219-225.
84. Sieber C, Kopf J, Hiepen C, Knaus P (2009) Recent advances in BMP receptor signaling. Cytokine Growth F R 20:343-355.
85. Silver J, Miller JH (2004) Regeneration beyond the glial scar. Nature Reviews Neuroscience 5:146-156.

86. Smith UM, Consugar M, Tee LJ, McKee BM, Maina EN, Whelan S, Morgan NV, Goranson E, Gissen P, Lilliquist S, Aligianis IA, Ward CJ, Pasha S, Punyashthiti R, Sharif SM, Batman PA, Bennett CP, Woods CG, McKeown C, Bucourt M, Miller CA, Cox P, Algazali L, Trembath RC, Torres VE, Attie-Bitach T, Kelly DA, Maher ER, Gattone VH, Harris PC, Johnson CA (2006) The transmembrane protein meckelin (MKS3) is mutated in Meckel-Gruber syndrome and the wpk rat. Nat Genet 38:191-196.
87. Sofroniew MV (2009) Molecular dissection of reactive astrogliosis and glial scar formation. Trends in neurosciences 32:638-647.
88. Sofroniew MV, Vinters HV (2010) Astrocytes: biology and pathology. Acta neuropathologica 119:7-35.
89. Stewart VC, Sharpe MA, Clark JB, Heales SJR (2000) Astrocyte-derived nitric oxide causes both reversible and irreversible damage to the neuronal mitochondrial respiratory chain. Journal of neurochemistry 75:694-700.
90. Thal SC, Wyschkon S, Pieter D, Engelhard K, Werner C (2008) Selection of endogenous control genes for normalization of gene expression analysis after experimental brain trauma in mice. J Neurotraum 25:785-794.
91. Tucker B, Klassen H, Yang L, Chen DF, Young MJ (2008) Elevated MMP expression in the MRL mouse retina creates a permissive environment for retinal regeneration. Invest Ophth Vis Sci 49:1686-1695.
92. Ueki Y, Reh TA (2012) Activation of BMP-Smad1/5/8 Signaling Promotes Survival of Retinal Ganglion Cells after Damage <italic>In Vivo</italic>. PloS one 7:e38690.
93. Voskuhl RR, Peterson RS, Song B, Ao Y, Morales LB, Tiwari-Woodruff S, Sofroniew MV (2009) Reactive astrocytes form scar-like perivascular barriers to leukocytes during adaptive immune inflammation of the CNS. J Neurosci 29:11511-11522.
94. Wang J, Li G, Wang Z, Zhang X, Yao L, Wang F, Liu S, Yin J, Ling EA, Wang L, Hao A (2012) High Glucose-Induced Expression of Inflammatory Cytokines and Reactive Oxygen Species in Cultured Astrocytes. Neuroscience 202:58-68.
95. Watanabe T, Raff MC (1988) Retinal astrocytes are immigrants from the optic nerve. Nature 332:834-837.
96. Wawersik S, Purcell P, Rauchman M, Dudley AT, Robertson EJ, Maas R (1999) BMP7 acts in murine lens placode development. Developmental biology 207:176-188.
97. Weinstein DC, Hemmati-Brivanlou A (1999) Neural induction. Annu Rev Cell Dev Bi 15:411-433.
98. Wilson SI, Edlund T (2001) Neural induction: toward a unifying mechanism. Nature neuroscience 4 Suppl:1161-1168.

99. Xiao Q, Du Y, Wu W, Yip HK (2010) Bone morphogenetic proteins mediate cellular response and, together with Noggin, regulate astrocyte differentiation after spinal cord injury. Exp Neurol 221:353-366.
100. Yamaguchi K, Nagai S, Ninomiya-Tsuji J, Nishita M, Tamai K, Irie K, Ueno N, Nishida E, Shibuya H, Matsumoto K (1999) XIAP, a cellular member of the inhibitor of apoptosis protein family, links the receptors to TAB1-TAK1 in the BMP signaling pathway. The EMBO journal 18:179-187.
101. Yanagisawa M, Takizawa T, Ochiai W, Uemura A, Nakashima K, Taga T (2001) Fate alteration of neuroepithelial cells from neurogenesis to astrocytogenesis by bone morphogenetic proteins. Neurosci Res 41:391-396.
102. Yuan L, Neufeld AH (2000) Tumor necrosis factor-alpha: a potentially neurodestructive cytokine produced by glia in the human glaucomatous optic nerve head. Glia 32:42-50.
103. Zhu HJ, Iaria J, Sizeland AM (1999) Smad7 differentially regulates transforming growth factor beta-mediated signaling pathways. Journal of Biological Chemistry 274:32258-32264.
104. Zode GS, Clark AF, Wordinger RJ (2007) Activation of the BMP canonical signaling pathway in human optic nerve head tissue and isolated optic nerve head astrocytes and lamina cribrosa cells. Invest Ophth Vis Sci 48:5058-5067.
105. Zuo J, Neubauer D, Dyess K, Ferguson TA, Muir D (1998) Degradation of chondroitin sulfate proteoglycan enhances the neurite-promoting potential of spinal cord tissue. Exp Neurol 154:654-662.

TABLES

Table 1 **List of primary antibodies used for western blot analysis**				
ANTIBODY	**COMPANY**	**CATALOGUE NUMBER**	**HOST SPECIES**	**DILUTION**
GFAP	DAKO	M0761	Mouse	1:500
Glutamine Synthetase	Millipore	MAB302	Mouse	1:500
phospho SMAD 1,5,8	Cell signaling	9511	Rabbit	1:1000
β-Tubulin	Sigma-Aldrich	T0198	Mouse	1:1000

Table 2 **List of primary antibodies used for fluorescence immunohistochemistry**				
ANTIBODY	**COMPANY**	**CATALOGUE NUMBER**	**HOST SPECIES**	**DILUTION**
GFAP	DAKO	Z0334	Rabbit	1:250
Glutamine Synthetase	Millipore	MAB302	Mouse	1:250
S100 β	Abcam	AB52642	Rabbit	1:250
Neurocan	R & D systems	AF5800	Sheep	1:100
BMP7	Santa Cruz	sc-73748	Rabbit	1:250
pSMAD1	Santa Cruz	sc-12353	Rabbit	1:100

Table 3 **List of primers used in qPCR**

Gene	Accession Number	Primer	Sequence	Product Length (bp)
GFAP1	NM_001131020.1	Forward	CCCTGGACATCGAGATCGCCACC	117
		Reverse	CTTTGGTGCTTTTGCCCCCTCGG	
GFAP2	NM_010277.3	Forward	TAGCCCTGGACATCGAGATCGCC	141
		Reverse	GGTGGCCTTCTGACACGGATTTGG	
Pax2	NM_011037.4	Forward	ACCCTGGCAGGAATGGTGCCT	70
		Reverse	AGGCGGTGTACTGGGGATGGC	
S100-β	NM_009115.3	Forward	GACTGCGCCAAGCCCACACC	142
		Reverse	TCCAGCTCGGACATCCCGGG	
NOS	NM_008712.2	Forward	TACGGGCATTGCTCCCTTCCGA	93
		Reverse	AACACCAAGCTCATGCGGCCT	
GS	NM_008131.3	Forward	GCGCTGCAAGACCCGTACCC	145
		Reverse	GGGGTCTCGAAACATGGCAACAGG	
VIM	NM_011701.4	Forward	AGGAAGCCGAAAGCACCCTGC	78
		Reverse	TCCGTTCAAGGTCAAGACGTGCC	
EGFR1	NM_207655.2	Forward	AAAGCGTACACTACGCCGCCTG	150
		Reverse	GTGCCAAATGCTCCCGAACCCA	
EGFR2	NM_007912.4	Forward	ACCTATGCCACGCCAACTGTACCT	82
		Reverse	TGAACGTACCCAGATGGCCACACTT	

Table 3 **List of primers used in qPCR (continued)**

Gene	Accession Number	Primer	Sequence	Product Length (bp)
TLR2	NM_011905.3	Forward	TGGAGCATCCGAAT TGCATCACCG	112
		Reverse	GCCACCAAGATCCAG AAGAGCCA	
TLR4	NM_021297.2	Forward	TGCCTGACACCAGGA AGCTTGA	102
		Reverse	AGGAATGTCATCAGG GACTTTGCTG	
B2M	NM_009735.3	Forward	TCGCGGTCGCTTCA GTCGTC	135
		Reverse	CATTCTCCGGTGG GTGGCGTG	
ACAN	NM_007424.2	Forward	GGCGTGCGCCCAT CATCAGAAA	86
		Reverse	TCGAGGCGTGTGG CGAAGAA	
PCAN	NM_001081306.1	Forward	ATCCCTGAGTGGG GAAGGCACA	96
		Reverse	AGCAGGGGATGCTG GGTGATGA	
NCAN	NM_007789.3	Forward	CCTGACAAGCGT CCATTCGCCA	90
		Reverse	ACTGTCCGGTCAT TCAGGCCGAT	
VCAN	NM_172955.1	Forward	TGGATTCCGCTCT CCCCAGGAA	119
		Reverse	ACTCTGCTTCGGC CTCCTCGAA	
TIMP1	NM_001044384.1	Forward	ACAGCCTTCTGCAA CTCGGACC	141
		Reverse	TGCGGCATTTCCC ACAGCCT	
TIMP2	NM_011594.3	Forward	TGCACCCGCAACAG GCGTTT	78
		Reverse	CGGAATCCAC CTCCTTCTCGCTCA	

Table 3 **List of primers used in qPCR (continued)**

Gene	Accession Number	Primer	Sequence	Product Length (bp)
TIMP3	NM_011595.2	Forward	TGACTCCCTGGCT TGGGCTTGT	147
		Reverse	TCTTTCCCACCACT TTGGCCCG	
TIMP4	NM_080639.3	Forward	AGCACTTCTGCCA CTCGGCTCTA	77
		Reverse	AGGGTCTTTGCTG GCAGGGACTAC	
MMP2	NM_008610.2	Forward	TGGCAAGGTGTG GTGTGCGA	133
		Reverse	AGAGTGTTCCAGC CCCATGGCA	
MMP3	NM_010809.1	Forward	TGGGTCTCCCTG CAACCGTGAA	141
		Reverse	TCTTCCTGGGAAA TCCTGGCTCCAT	
MMP9	NM_013599.2	Forward	TGTGCCCTGGAA CTCACACGAC	135
		Reverse	ACGTCGTCCACCT GGTTCACCT	
MMP11	NM_008606.2	Forward	ACTGACTGGCGA GGGGTACCTT	128
		Reverse	GCAGATGGACCC CATGTTTGCTGT	
MMP12	NM_008605.3	Forward	GCTGTCTTTGACCC ACTTCGCCA	88
		Reverse	GGTCCATGAGCTC CTGCCTCACAT	
MMP13	NM_008607.2	Forward	GCGTGGCTGGAA CCACATGGAA	128
		Reverse	GCAGATGGACCCCA TGTTTGCTGT	
MMP14	NM_008608.3	Forward	TGGGCCCAAGGCAG CAACTT	89
		Reverse	CGTTGTGTGTGGG TACGCAGGT	

Table 3 **List of primers used in qPCR (continued**)

Gene	Accession Number	Primer	Sequence	Product Length (bp)
BMP2	NM_007553.2	Forward	AATGGACGTGCCCC CTAGTGCT	106
		Reverse	AGGACCTGGGGAAG CAGCAACA	
BMP4	NM_007554.2	Forward	AGCCGAGCCAACAC TGTGAGGA	78
		Reverse	AGCAGAGCTCTCAC TGGTCCCT	
BMP6	NM_007556.2	Forward	TTCCTCAACGACGC GGACATGG	85
		Reverse	TGTGGTGTCGTTGAT GTGGGGAGA	
BMP7	NM_007557.2	Forward	TCCTCACTGACGCC GACATGGT	97
		Reverse	AACCGGAACTCCCG ATGGTGGT	
SMAD1	NM_008539.3	Forward	TACCCTCACTCCCC AACCAGCTCA	143
		Reverse	GGAGGCGCCATCAT GTTCGTGT	
SMAD5	NM_001164041.1	Forward	TCCCTCGCTGCGCT AAACTTTGT	137
		Reverse	AAGCGTGGCTCGCA GGTGAA	
SMAD6	NM_008542.3	Forward	AGGCCACCAACTCC CTCATCACT	70
		Reverse	TTGGTGGCATCCGG AGACATGC	
SMAD7	NM_001042660.1	Forward	CTGCAGGCTGTCC AGATGCTGT	132
		Reverse	ATGCCACCACGCAC CAGTGT	
SMAD8	NM_019483.4	Forward	ATGCCGCACAACGC CACCTA	88
		Reverse	ACTGCGGAAACAC ATGGCCTGG	

Table 3 **List of primers used in qPCR (continued)**				
Gene	Accession Number	Primer	Sequence	Product Length (bp)
ID1	NM_010495.2	Forward	TCAGCACCCTGAA CGGCGAGAT	70
		Reverse	ATGCGATCGTCGG CTGGAACA	
ID3	NM_008321.2	Forward	ACCTTCAGGTGGT CCTGGCAGA	134
		Reverse	ACGACCGGGTCA GTGGCAAAA	
MSX2	NM_013601.2	Forward	ACCGCCTCGGTC AAGTCGGAAA	116
		Reverse	TGTTTCCTCAGGG TGCAGGTGGT	

Table 4 **Panel of markers used for assessment of reactivity via qPCR**

REACTIVITY PANEL
• Glial fibrillary acidic protein variant 2 – GFAP2
• PAX2
• S100-β
• EGFR1
• TLR4
• Phosphacan – PCAN
• Neurocan - NCAN
• Tissue inhibitor of metalloproteinases 2 – TIMP2
• Matrix metalloproteinase 9 – MMP9
• Matrix metalloproteinases 11 – MMP11
• Matrix metalloproteinase 14 – MMP14

FIGURES

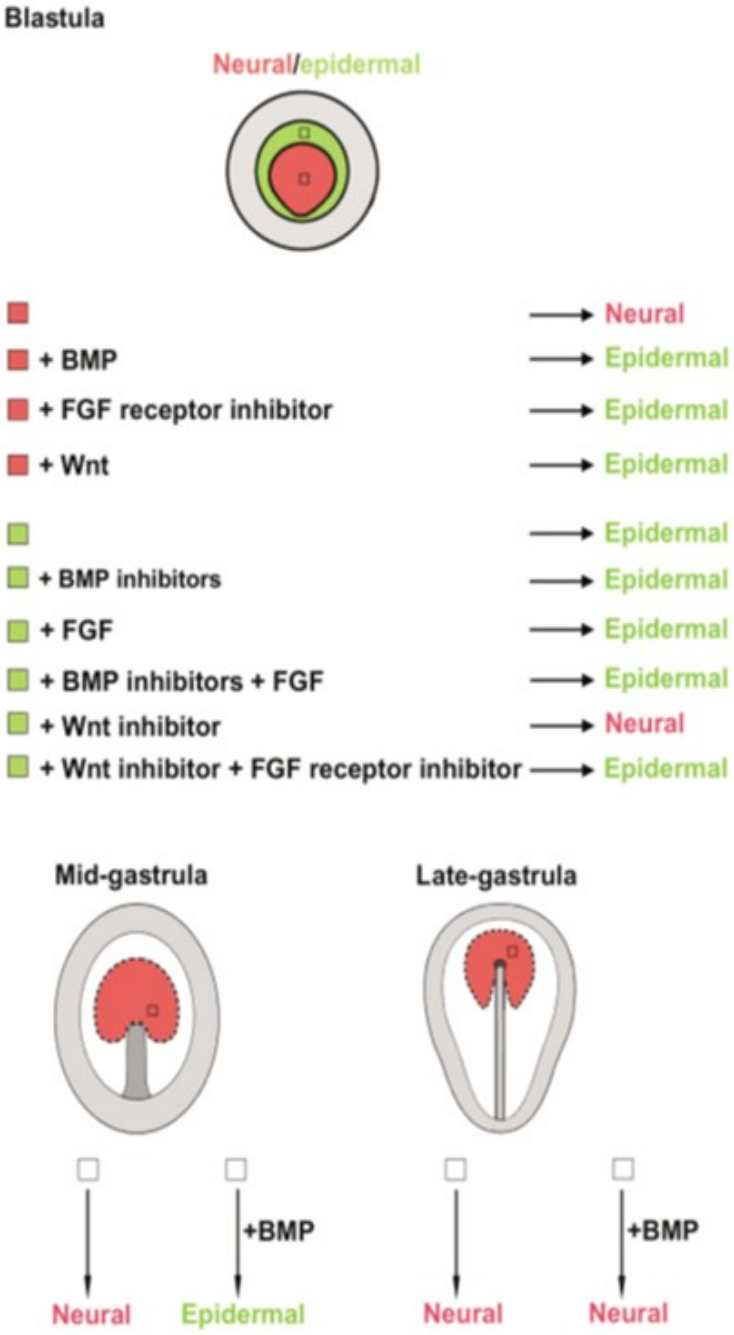

Fig. 1 **Specification map of the blastula stage chick embryos**: the neurogenic (red) region and the epidermal (green) region; and the effects of different growth factors on the lineage determination (Wilson and Edlund, 2001)

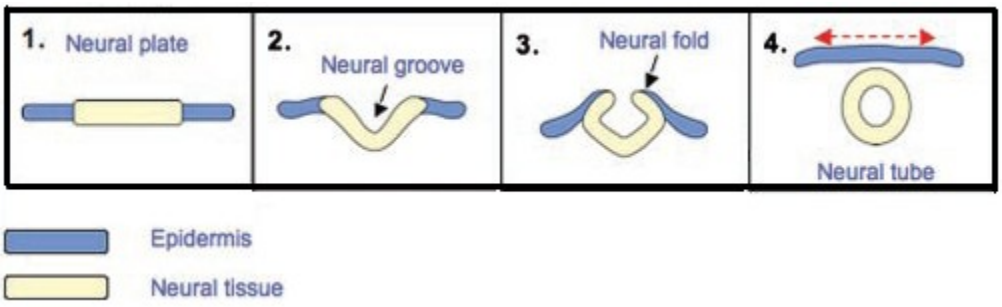

Fig. 2 **Primary neurulation in amniotes**: Development of the neural tube from the neural plate (Harrington et al., 2009)

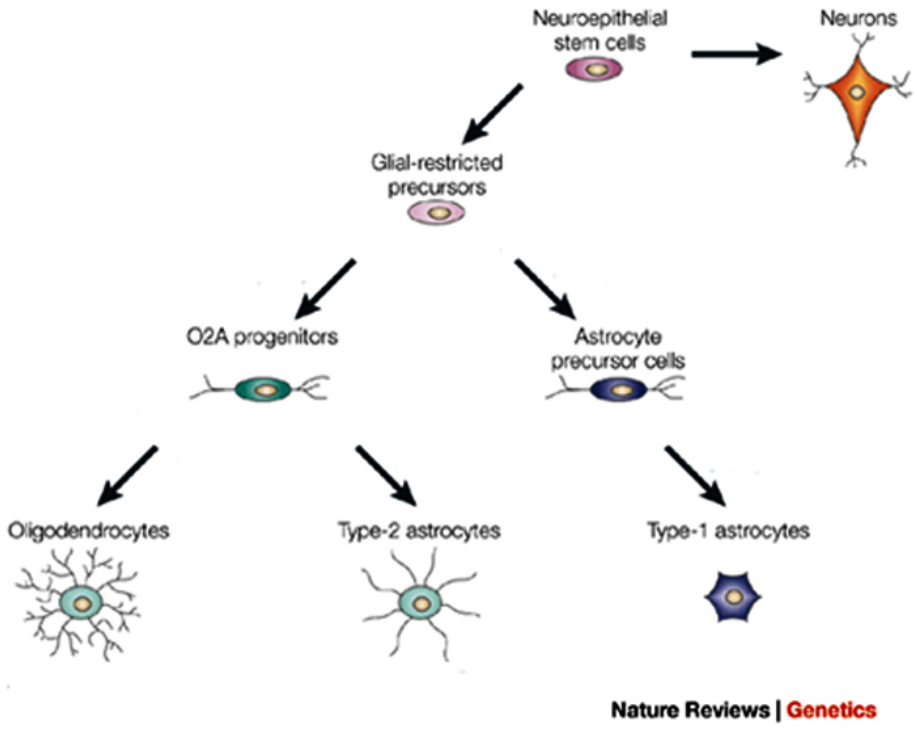

Fig. 3 **Development of astrocytes from neuroepithelial precursor cells**: Progression and changes in the differentiation of the neuroepithelial precursor cells during development (Modified from Holland E. 2001, review)

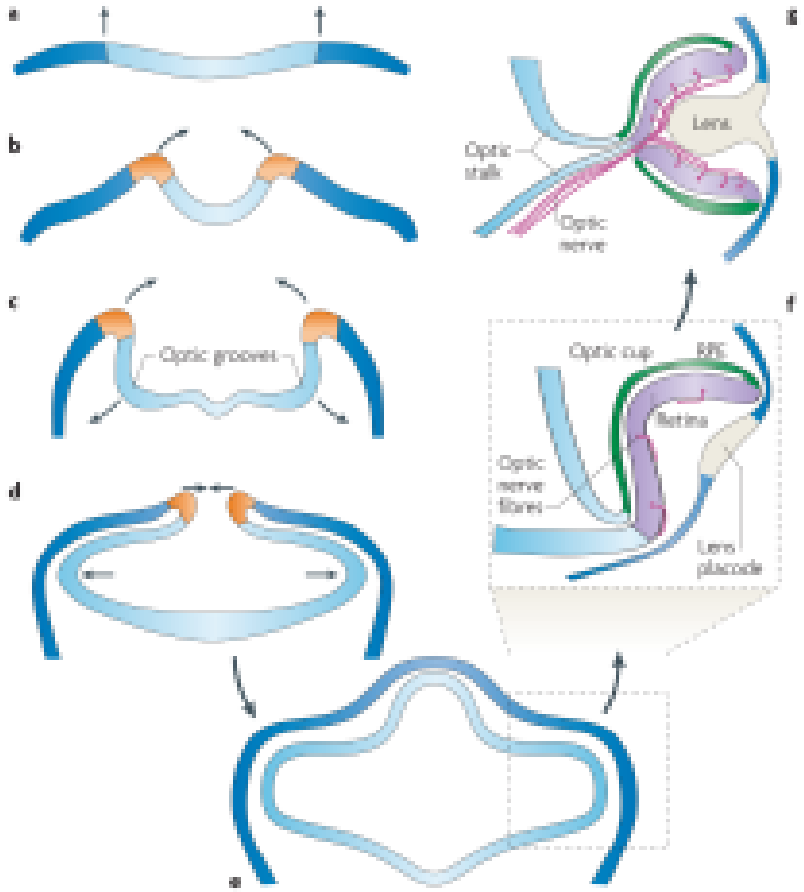

Fig. 4 **Development of the vertebrate eye**: (a) The neural plate, (b) The neural plate begins to fold upwards and inwards forming the neural tube,(c) The eye field in the neural plate spilts and forms the optic grooves, (d) As the ends of the folds move in closer, the optic groove evaginates, (e) After the closure of the neural tube, the ends of the optic vesicle come in close proximity of the outer head ectoderm and induces the lens placode, (f) The optic vesicle folds on itself, now called the optic cup, forming the retina proximal to the lens, retinal pigmented epithelium distal to the lens and the ventral optic stalk, (g) The optic cup enlarges and eventually seals off the choroid fissure and enclosing the optic nerve (Lamb et al., 2007)

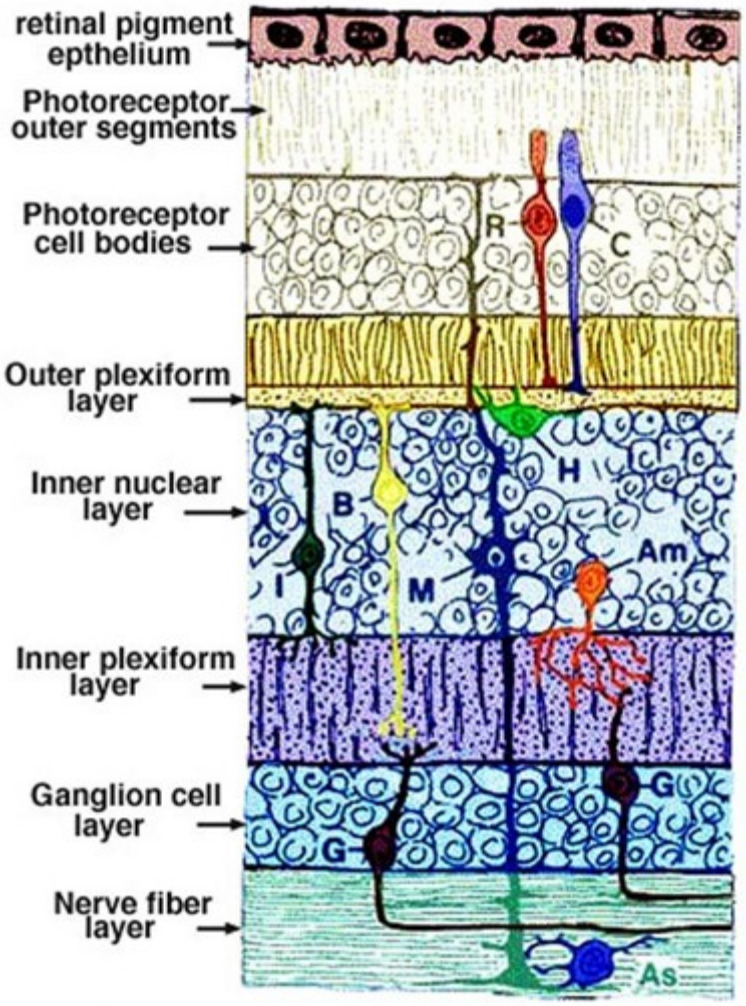

Fig. 5 **Layers of the mature vertebrate retina**: Organization of the mature retina along with the different cell types present (http://webvision.med.utah.edu/book/part-i-foundations/gross-anatomy-of-the-ey/)

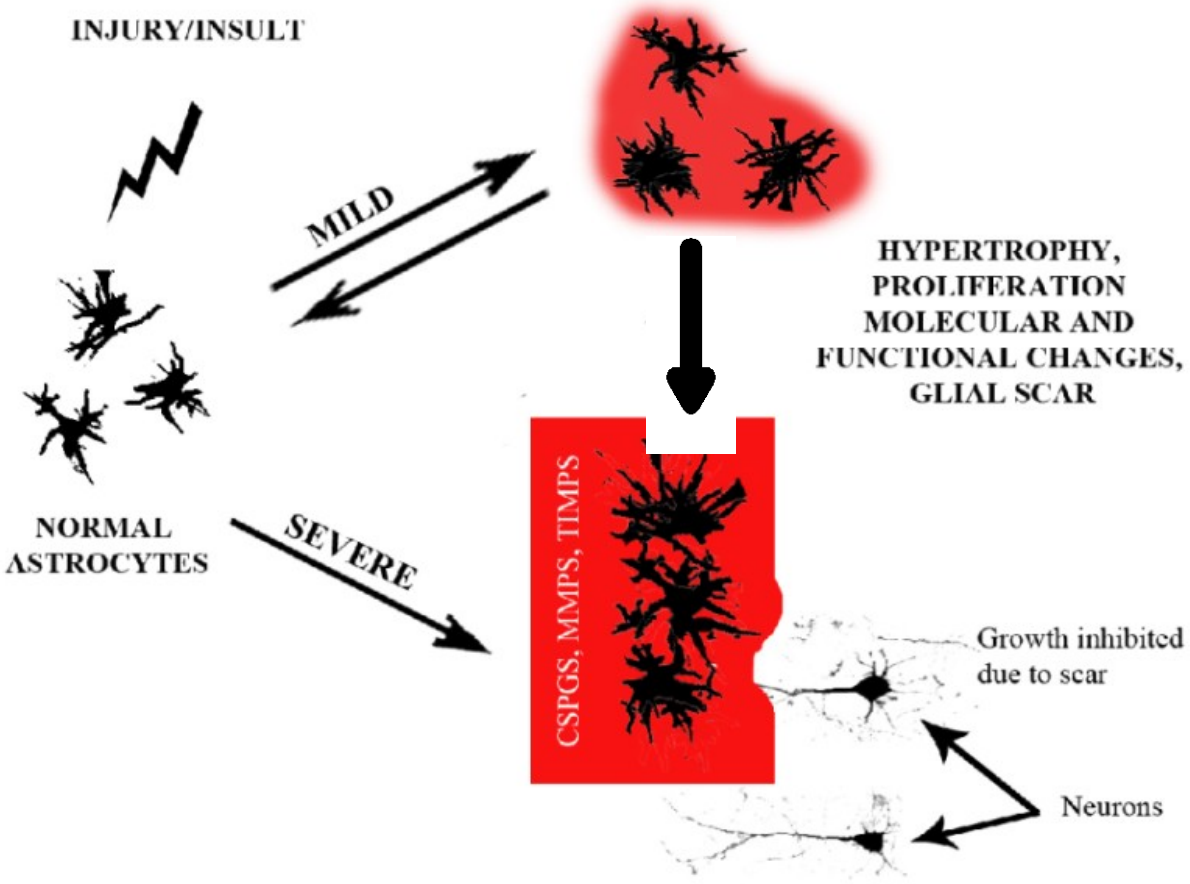

Fig. 6 **Summary of reactive gliosis**: Changes in molecular and morphological characteristics of astrocytes due to an injury or disease of the nearby neurons, altering the functions of astrocytes by inter and intra cellular signaling molecules. Based on the extent of the injury, the gliosis can be either mild or severe

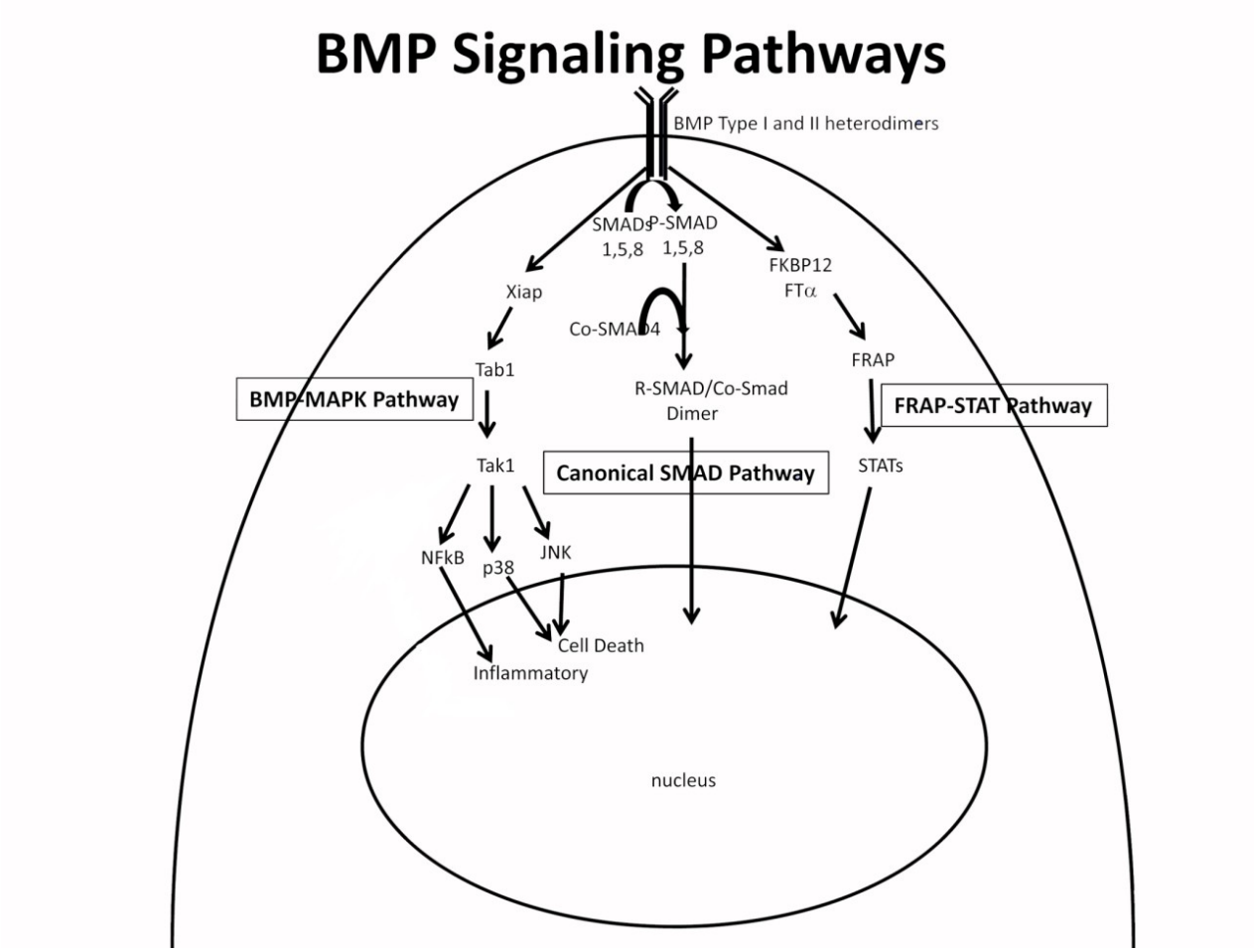

Fig. 7 **The BMP pathway**: Signaling through the BMP pathway follows either the canonical (SMAD dependent) pathway or the non canonical (SMAD independent) pathway

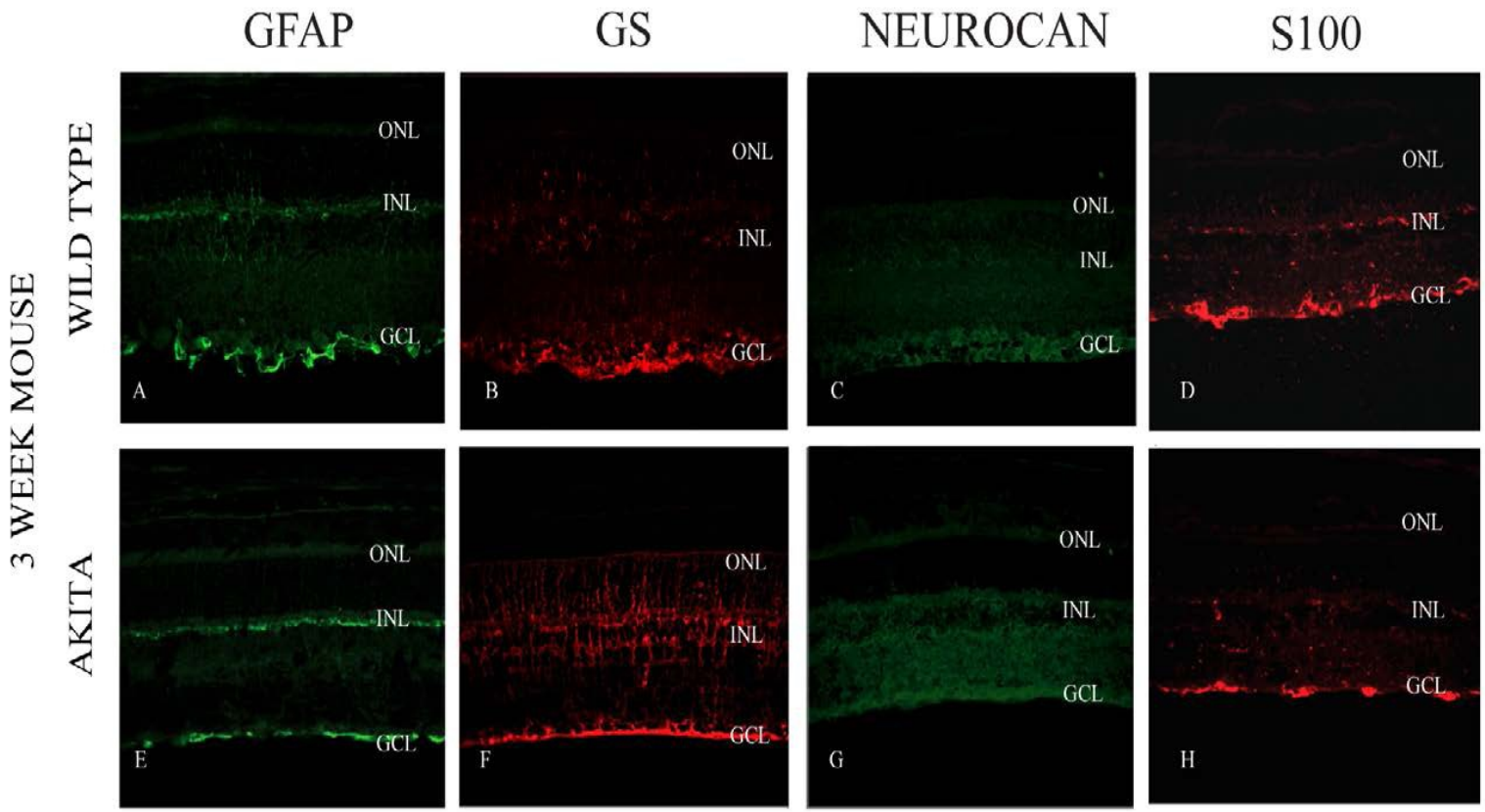

Fig. 8 **Characterization of reactivity *in vivo* in the 3 week Ins2^{Akita} mouse**: IHC of sections through WT and 3 week Ins2^{Akita} labelled for GFAP (A, E), glutamine synthetase (B, F), neurocan (C, G) and S100 (D, H). At 3 weeks, there are no detectable differences in the expression pattern GFAP, S100 or neurocan in WT (A,C, D) and Ins2^{Akita} (E, G , H). There was however, a detectable increase in glutamine synthetase in Ins2^{Akita} (F) in comparison to the WT (B).ONL: outer nuclear layer; INL: inner nuclear layer; GCL; ganglion cell layer

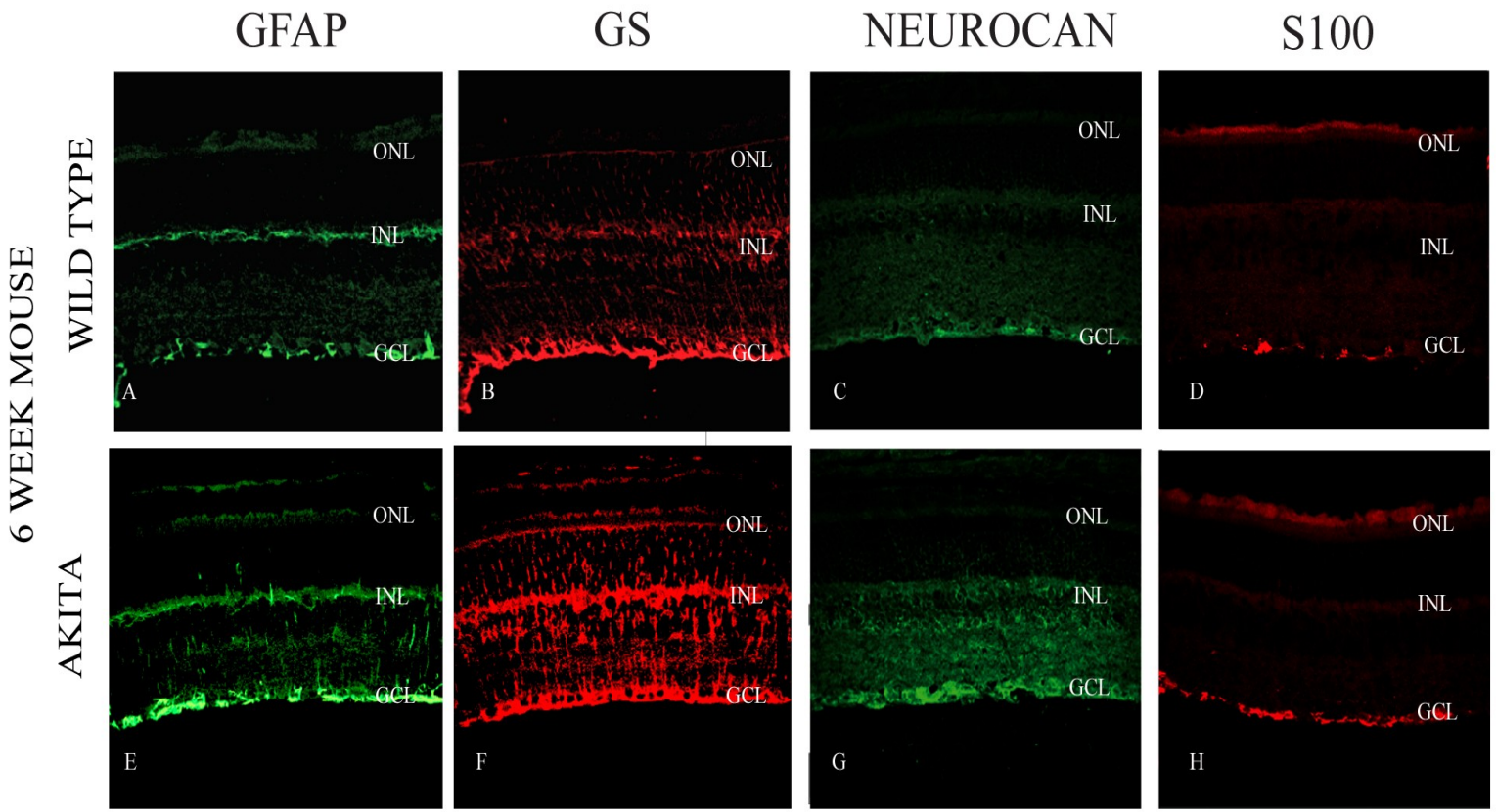

Fig. 9 **Characterization of reactivity *in vivo* in 6 week Ins2^{Akita} mouse**: IHC of sections through WT and 6 week Ins2^{Akita} labelled for GFAP (A, E), glutamine synthetase (B, F), neurocan (C, G) and S100 (D, H). At the 6 week stage, we observe detectable differences in the expression pattern GFAP, GS, S100 and neurocan in WT (A,B, C, D) and Ins2^{Akita} (E, F, G, H). ONL: outer nuclear layer; INL: inner nuclear layer; GCL; ganglion cell layer

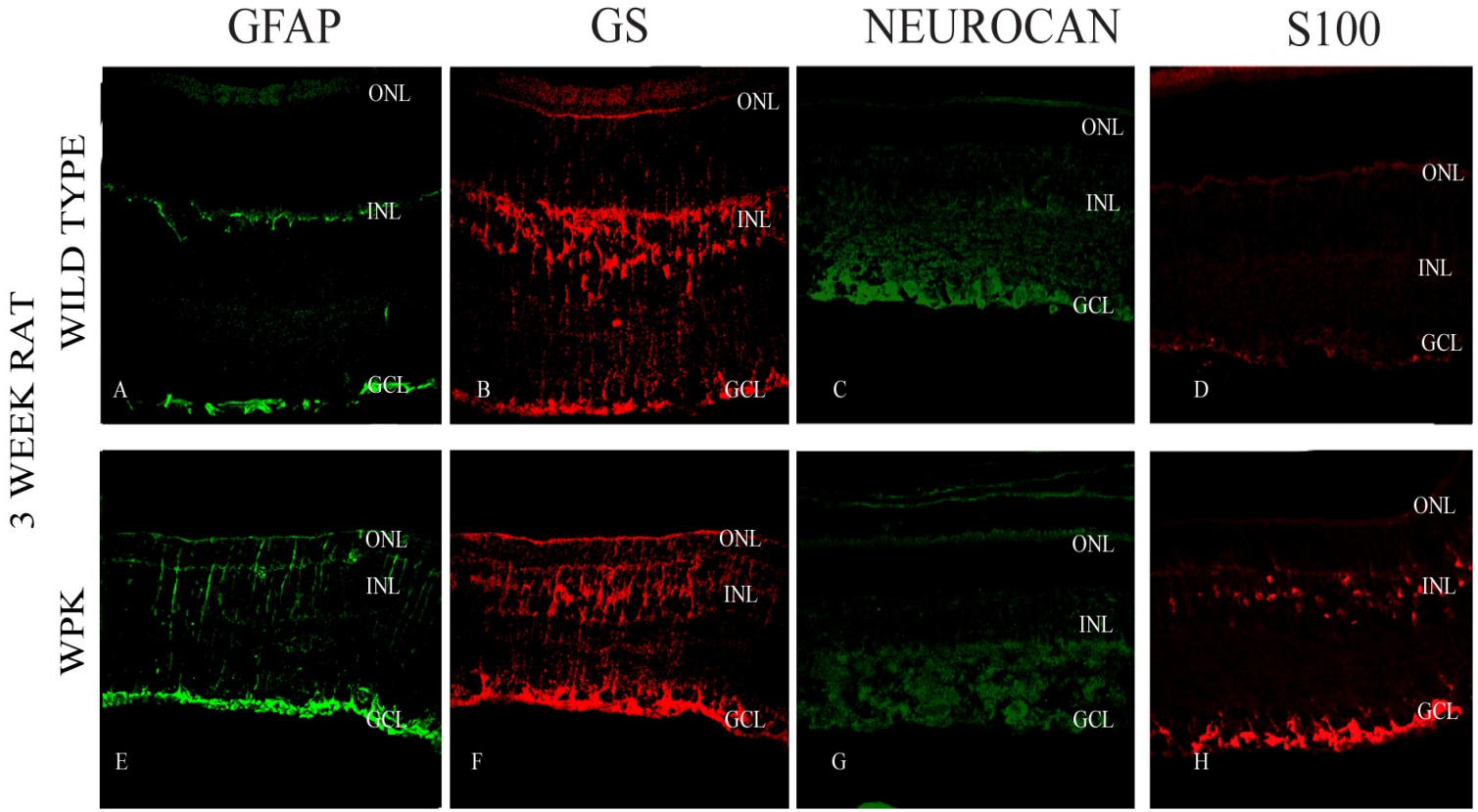

Fig. 10 **Characterization of reactivity *in vivo* in 3 week WPK rat**: IHC of sections through WT and 3 week WPK labelled for GFAP (A, E), glutamine synthetase (B, F), neurocan (C, G) and S100 (D, H). In the rat, we observe detectable differences in the expression pattern GFAP, GS and S100 in WT (A,B, D) and WPK (E, F, H). There was no detectable difference in the expression pattern of neurocan between the WT (C) and WPK (G). ONL: outer nuclear layer; INL: inner nuclear layer; GCL; ganglion cell layer

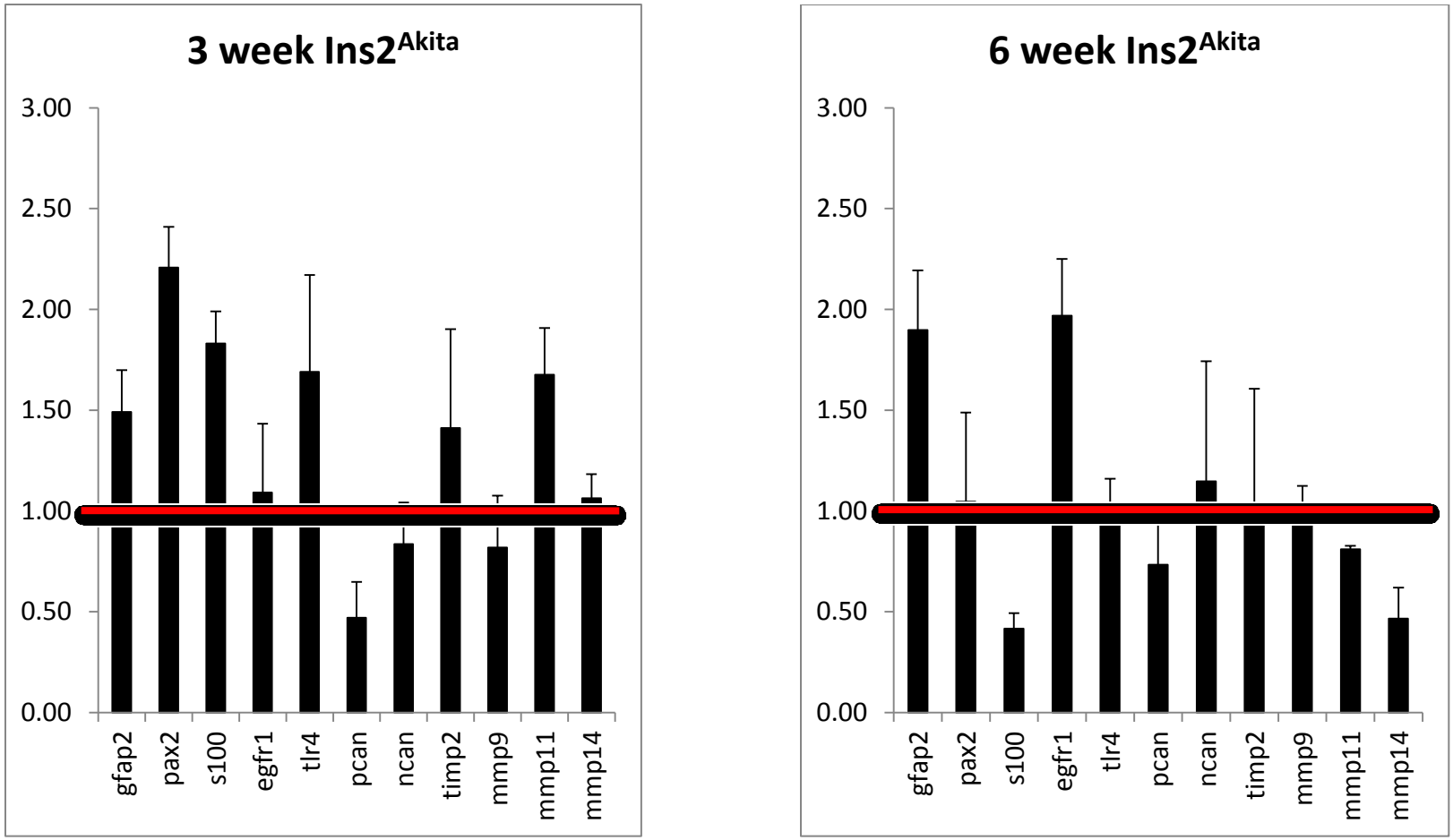

A. B.

Fig. 11 **Characterization of reactivity *in vivo* for reactivity markers**: qPCR analysis for levels of RNA for markers of reactivity in 3 week $Ins2^{Akita}$ (A) and 6 week $Ins2^{Akita}$ (B) mouse when normalized to wild type mouse

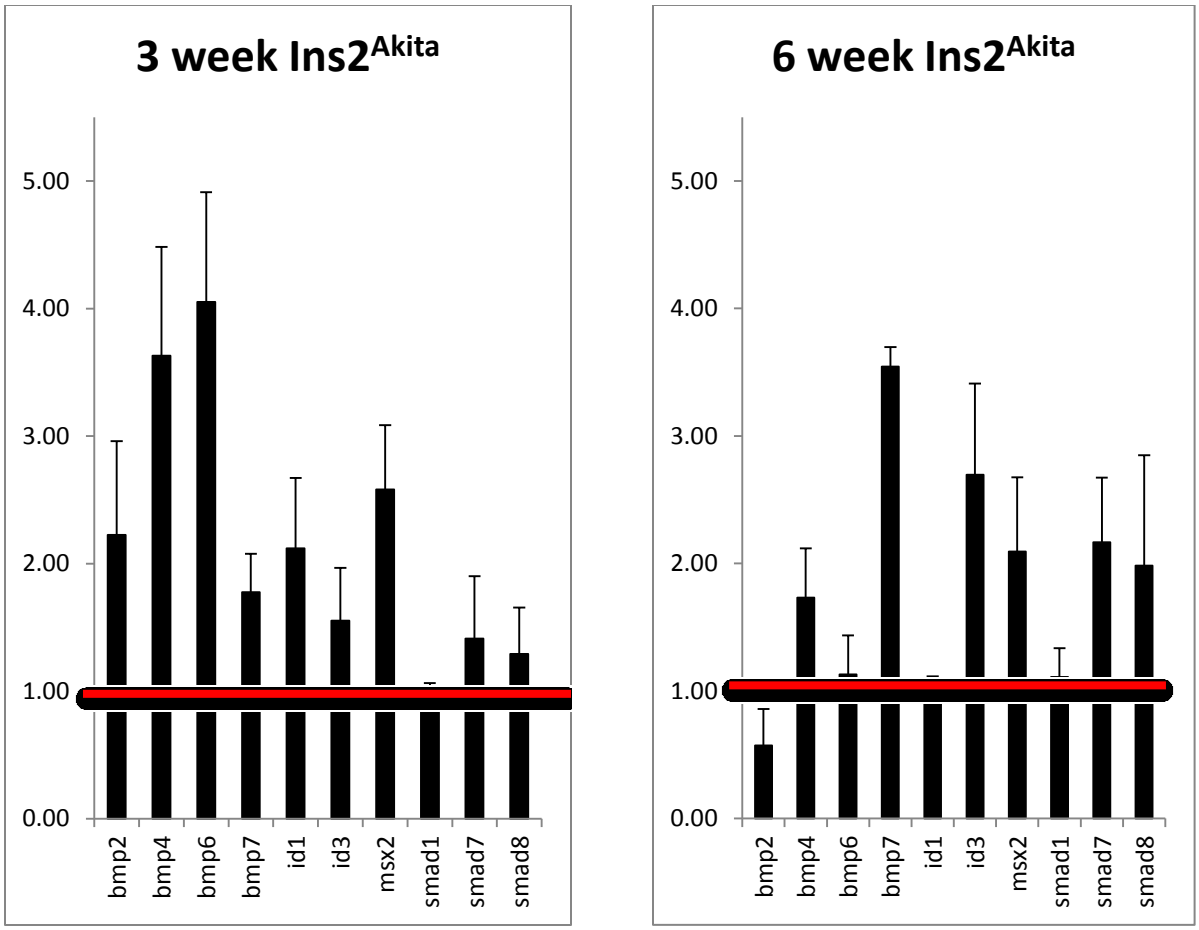

A. B.

Fig. 12 **BMP molecules and signaling components in whole mouse retinas**: qPCR analysis for levels of RNA for BMP molecules and downstream components of reactivity in 3 week $Ins2^{Akita}$ mouse (A) and 6 week $Ins2^{Akita}$ mouse (B) when normalized to wild type mouse

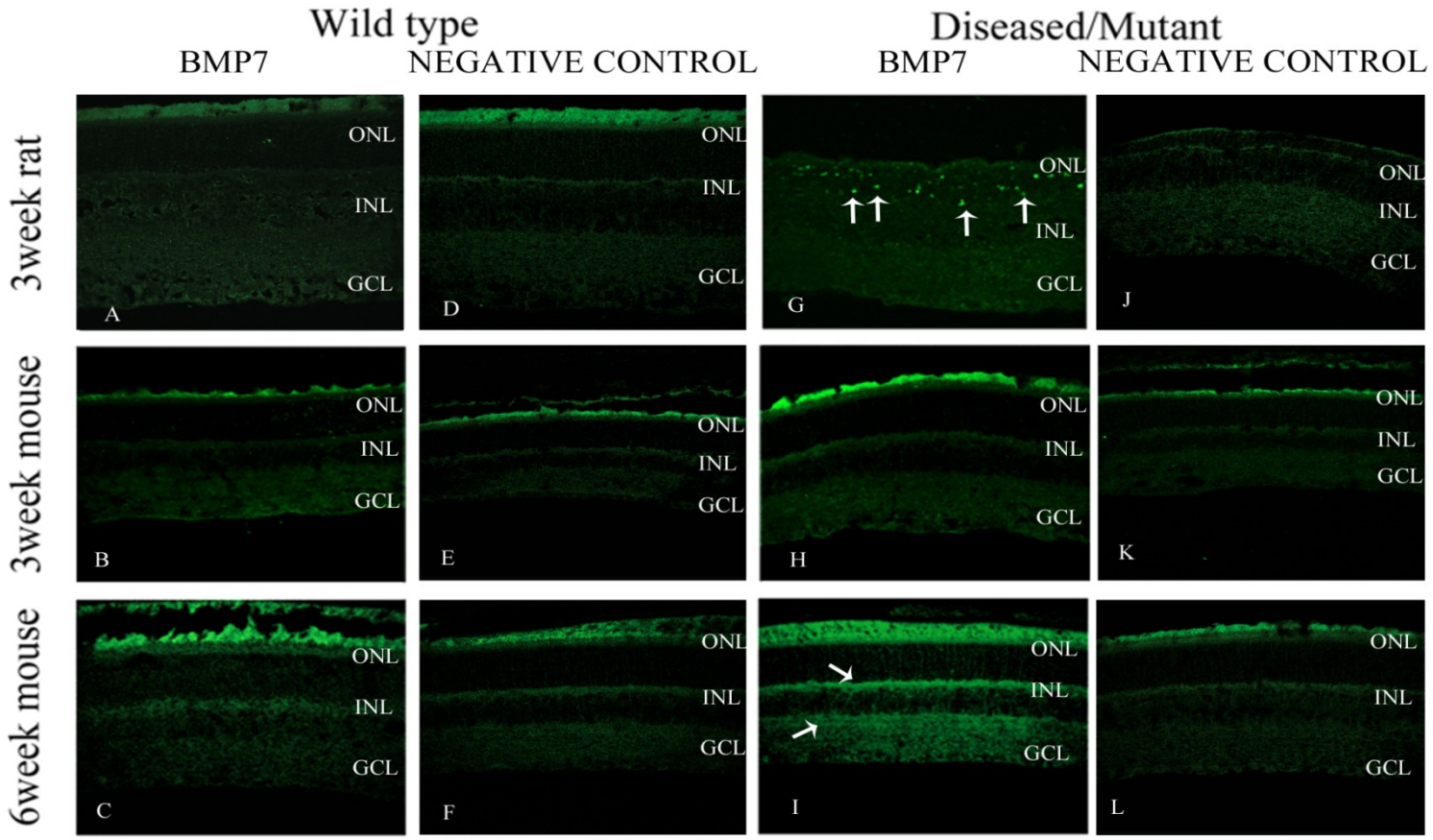

Fig. 13 **Characterization of BMP7 signaling *in vivo***: IHC staining of WT and WPK rat (A, G) and WT and $Ins2^{Akita}$ (B, C, H, I) mouse for BMP7.Detectable differences in the expression pattern of BMP7 is observed in the 3 week WPK rat (G) in the outher nuclear layer and in 6 week $Ins2^{Akita}$ (I) in the inner nuclear layers when compared to their WT (A, C). ONL: outer nuclear layer; INL: inner nuclear layer; GCL; ganglion cell layer

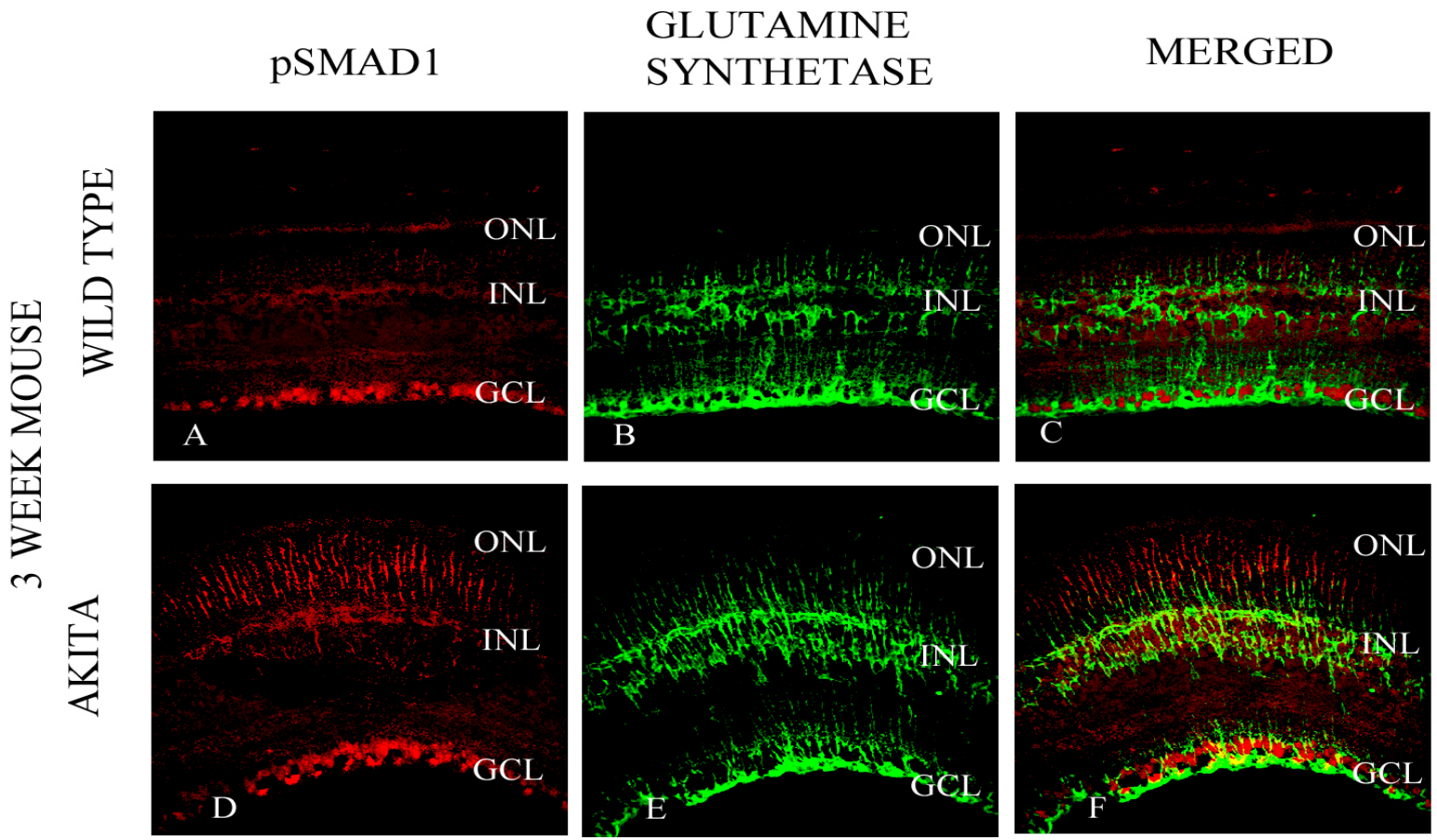

Fig. 14 **pSMAD1 and glutamine synthetase double labeling in 3 week wild type and Ins2^{Akita} mouse retinas**: The 3 week Ins2^{Akita} does show a detectable increase in pSMAD1 labeling, specifically in the process of glial cells in outer plexiform layers as observed in the merged images of pSMAD and GS(F) when compared to the WT (C). ONL: outer nuclear layer; INL: inner nuclear layer; GCL; ganglion cell layer

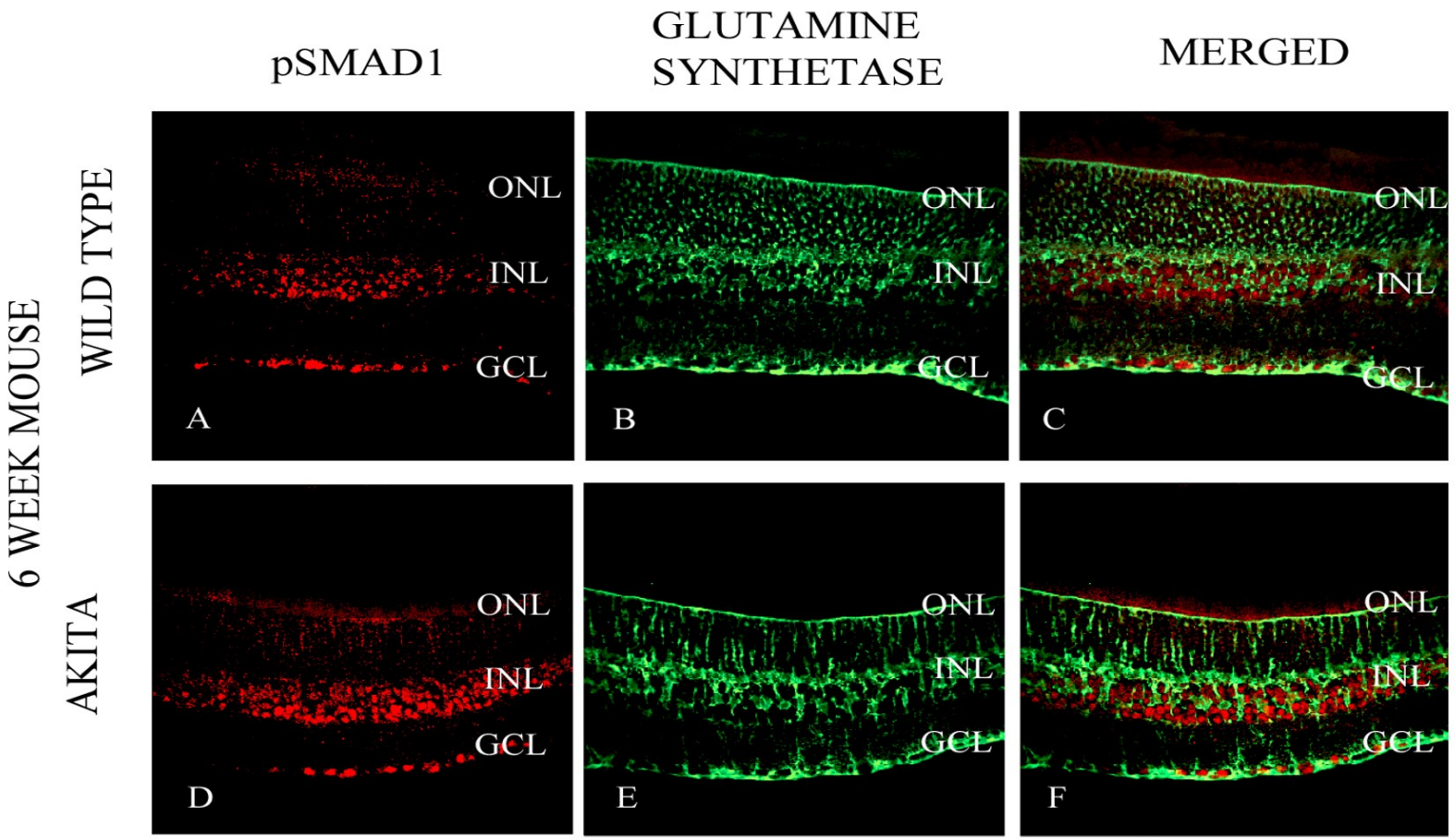

Fig. 15 **pSMAD1 and glutamine synthetase double labeling in 6 week wild type and Ins2^{Akita} mouse retinas**: The 6 week Ins2^{Akita} which was previously characterized to have reactive astrocytes does show a detectable increase in pSMAD1 labeling, specifically in the inner nuclear layer(D, F) when compared to the WT (A, C). ONL: outer nuclear layer; INL: inner nuclear layer; GCL; ganglion cell layer

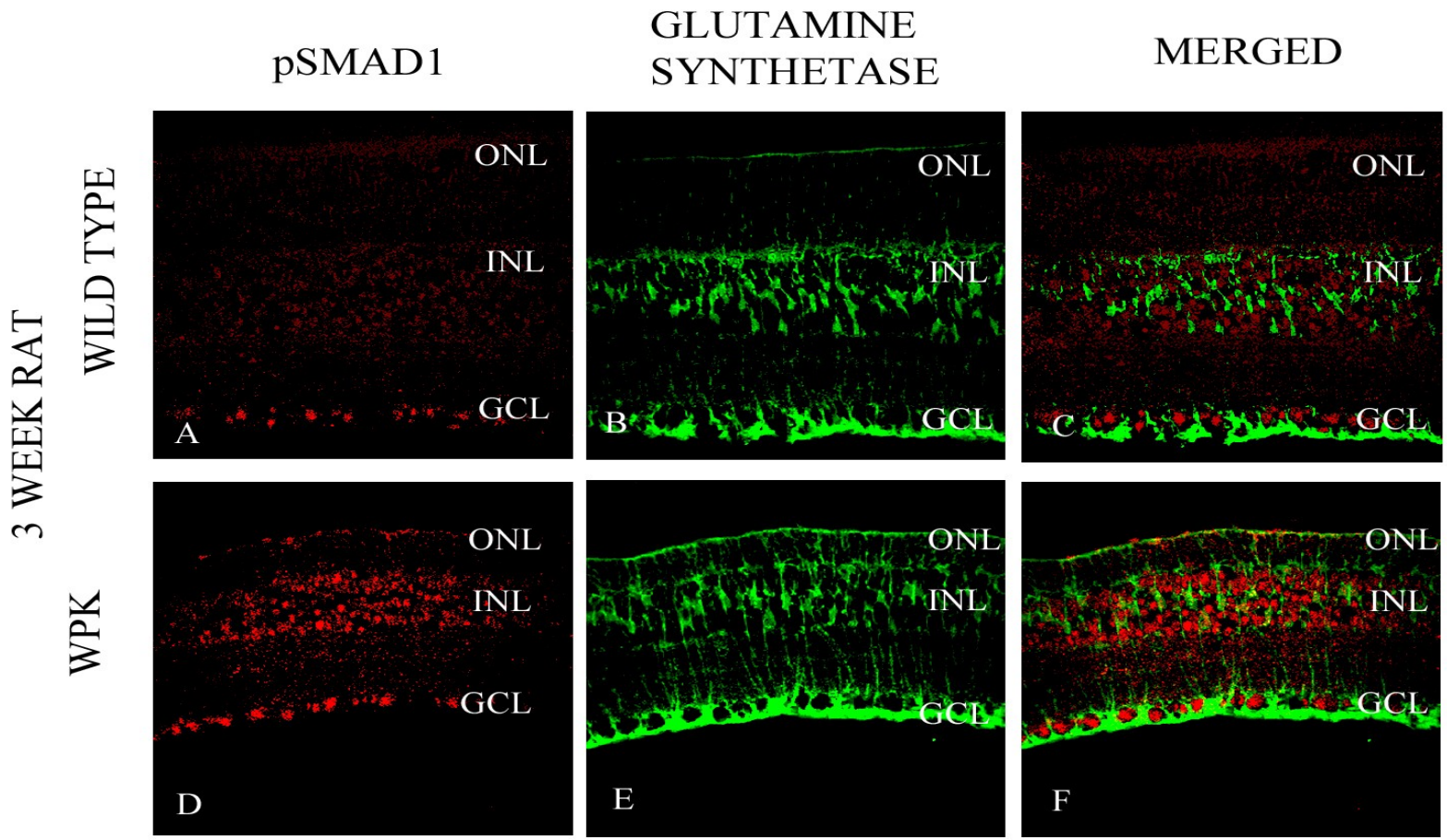

Fig. 16 **pSMAD1 and glutamine synthetase double labeling in 3 week wild type and WPK rat retinas**: The 3 week WPK, previously characterized to have reactive astrocytes does show a detectable increase in pSMAD1 labeling, specifically in the inner nuclear layer(D, F) when compared to the WT (A, C). ONL: outer nuclear layer; INL: inner nuclear layer; GCL; ganglion cell layer

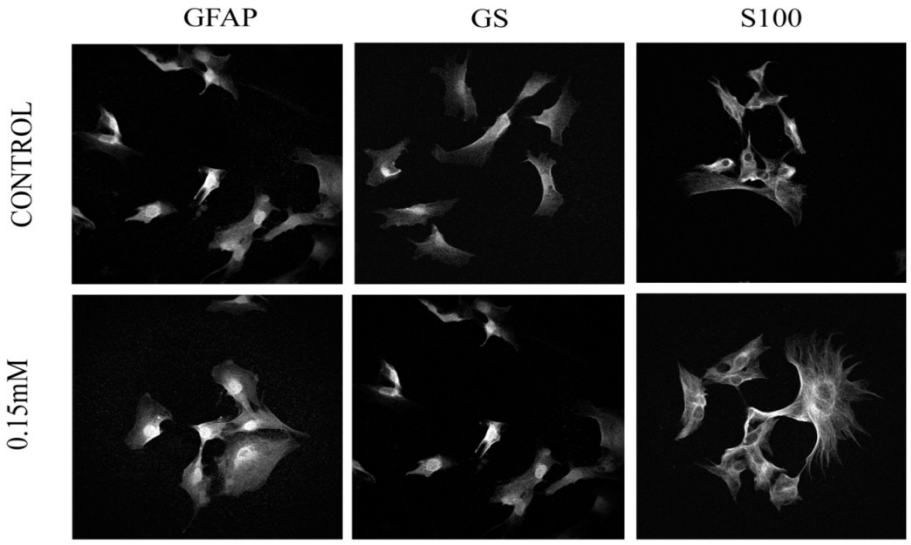

Fig. 17 **ICC of reactivity *in vitro***: Immunocytochemistry of peroxynitrite treated cells with antibodies against GFAP, GS and S100 shows more intense staining in the peroxynitrite treated cells

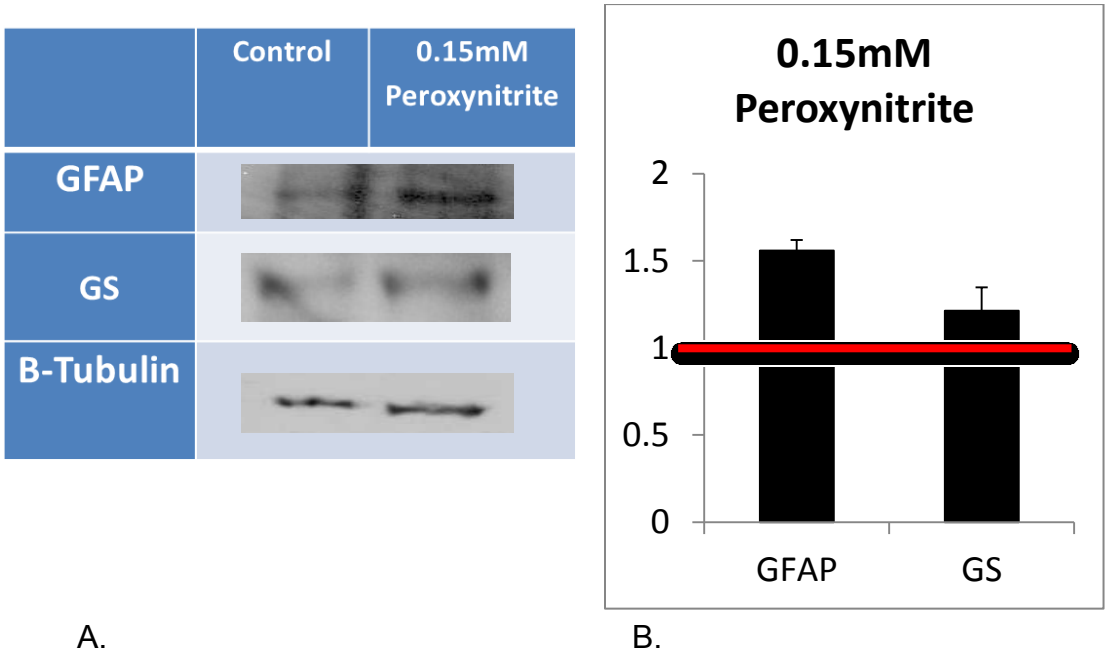

A. B.

Fig.18 **Characterization of reactivity *in vitro* via western blot**: (A) Western blot analysis of 0.15mM peroxynitrite treated cells compared to the control treatments for GFAP and beta tubulin. (B) Densitometric analysis of the blots normalized to the control treatments. β-Tubulin used as the loading control

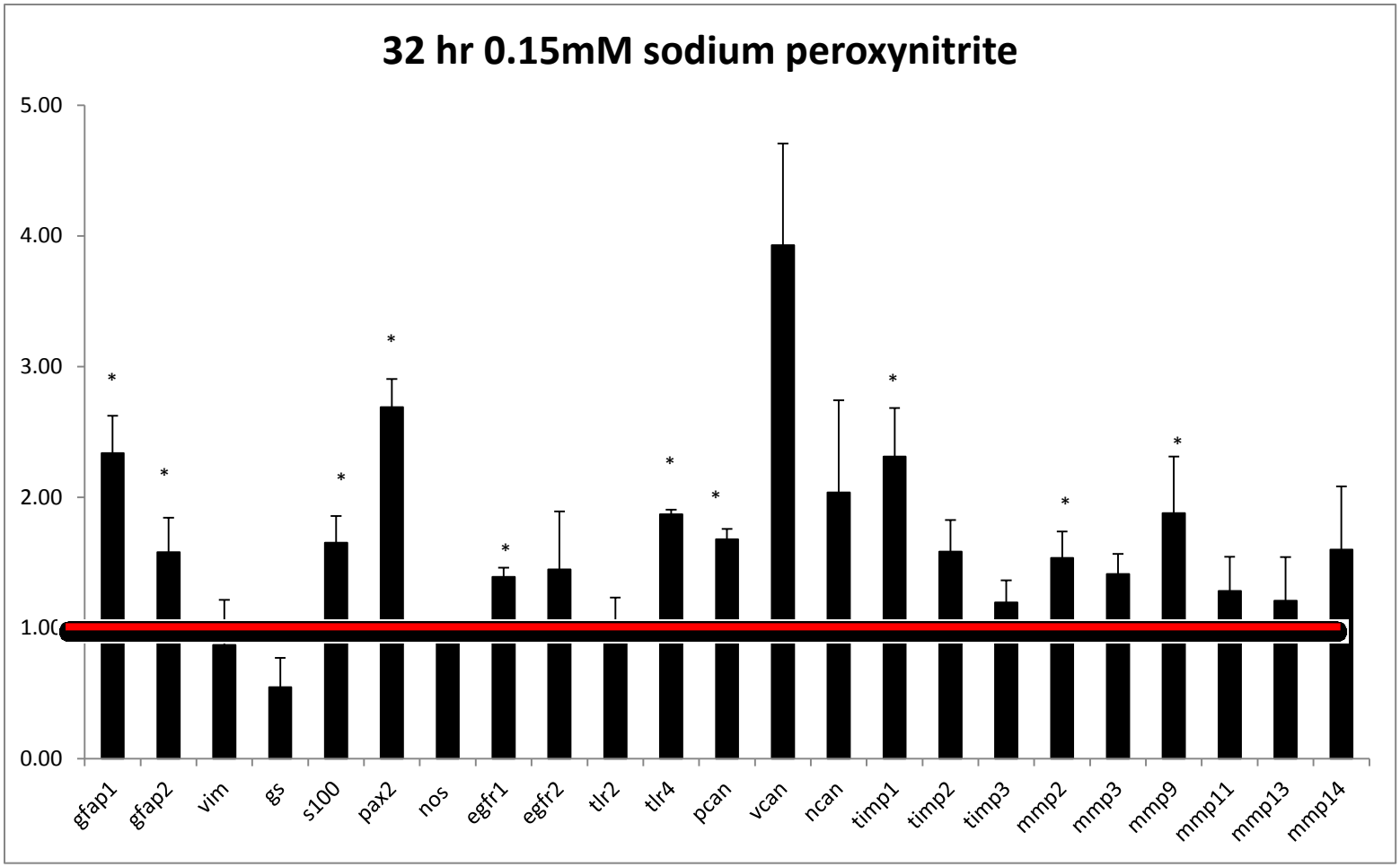

Fig. 19 **Reactivity of mouse retinal astrocytes *in vitro* due to sodium peroxynitrite**: qPCR data depicting markers showing change in levels of mRNA in astrocyte cells exposed to 0.15 mM sodium peroxynitrite for 32 hours normalized to the control treatment (* = *p value* < *0.05*)

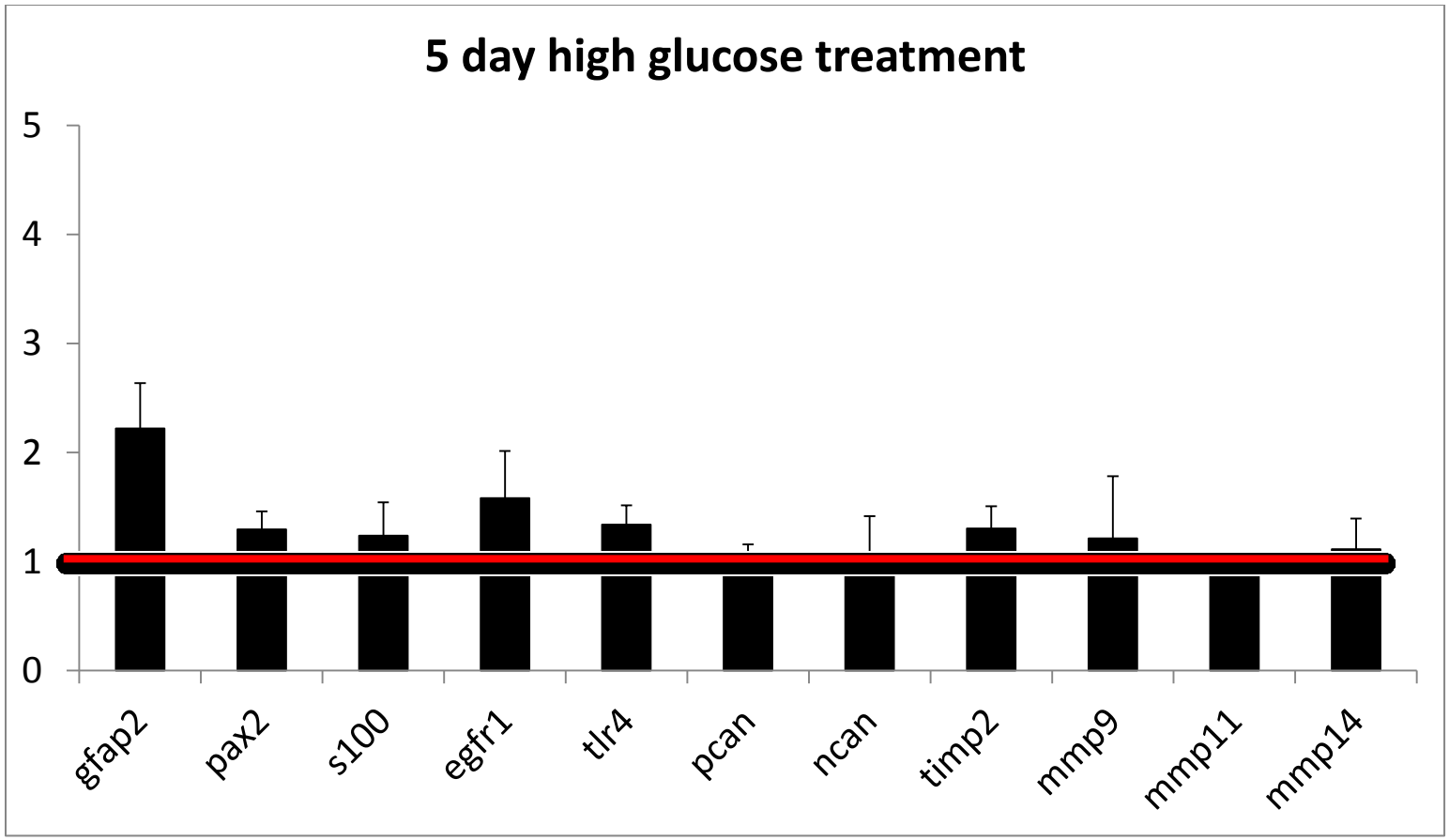

Fig. 20 **Reactivity of mouse retinal astrocytes *in vitro* due to high glucose DMEM**: qPCR data depicting markers showing change in levels of mRNA in astrocyte cells exposed to 40 mM glucose in DMEM for 5 days normalized to the control 5 mM low glucose treatment

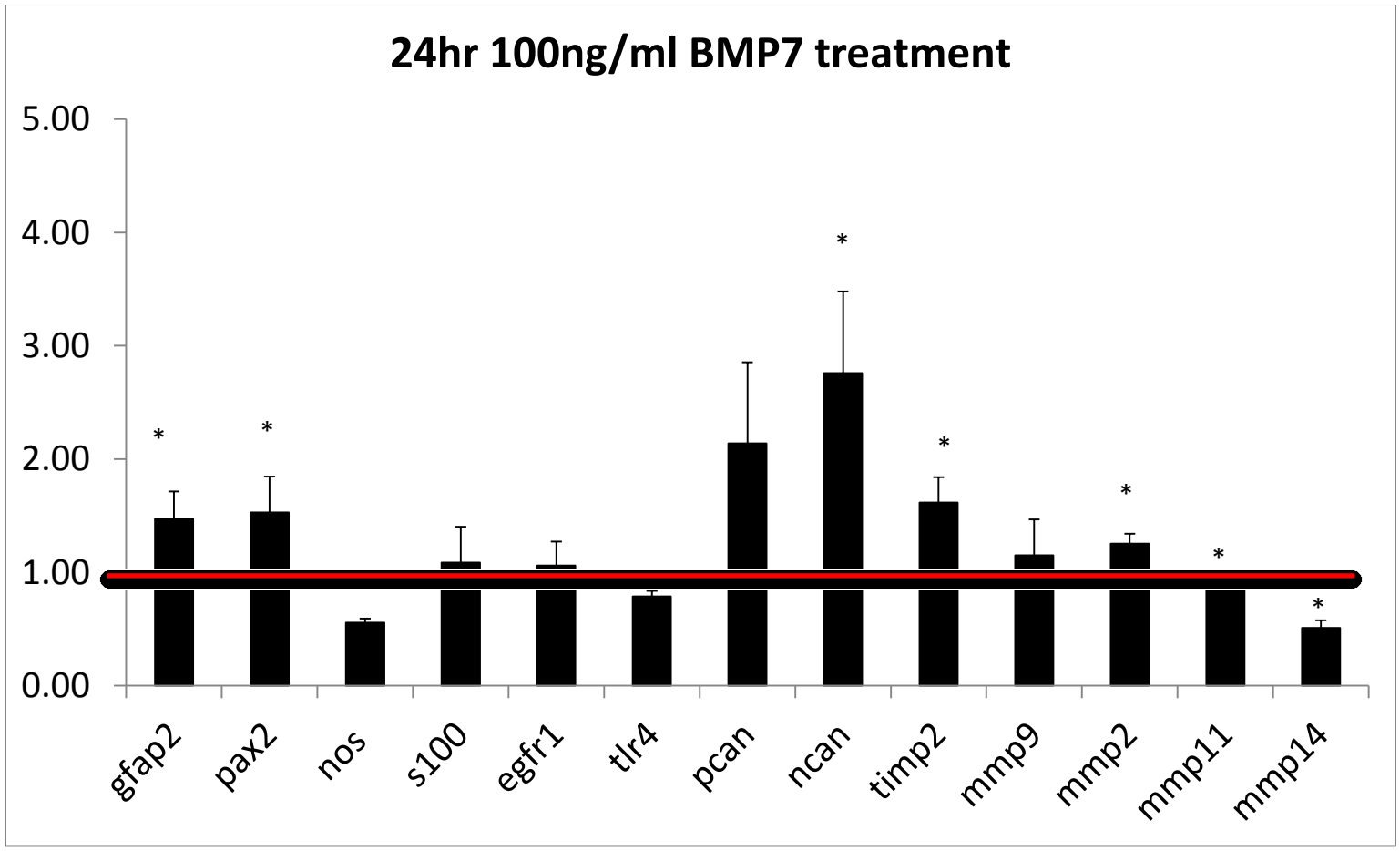

Fig. 21 **Effect of BMP7 on retinal astrocyte cells**: (A) qPCR data depicting markers which showed statistically significant change in levels of mRNA in astrocyte cells exposed to 100ng/ml BMP7 for 24 hours normalized to the control treatments (* = *p value* < *0.05*)

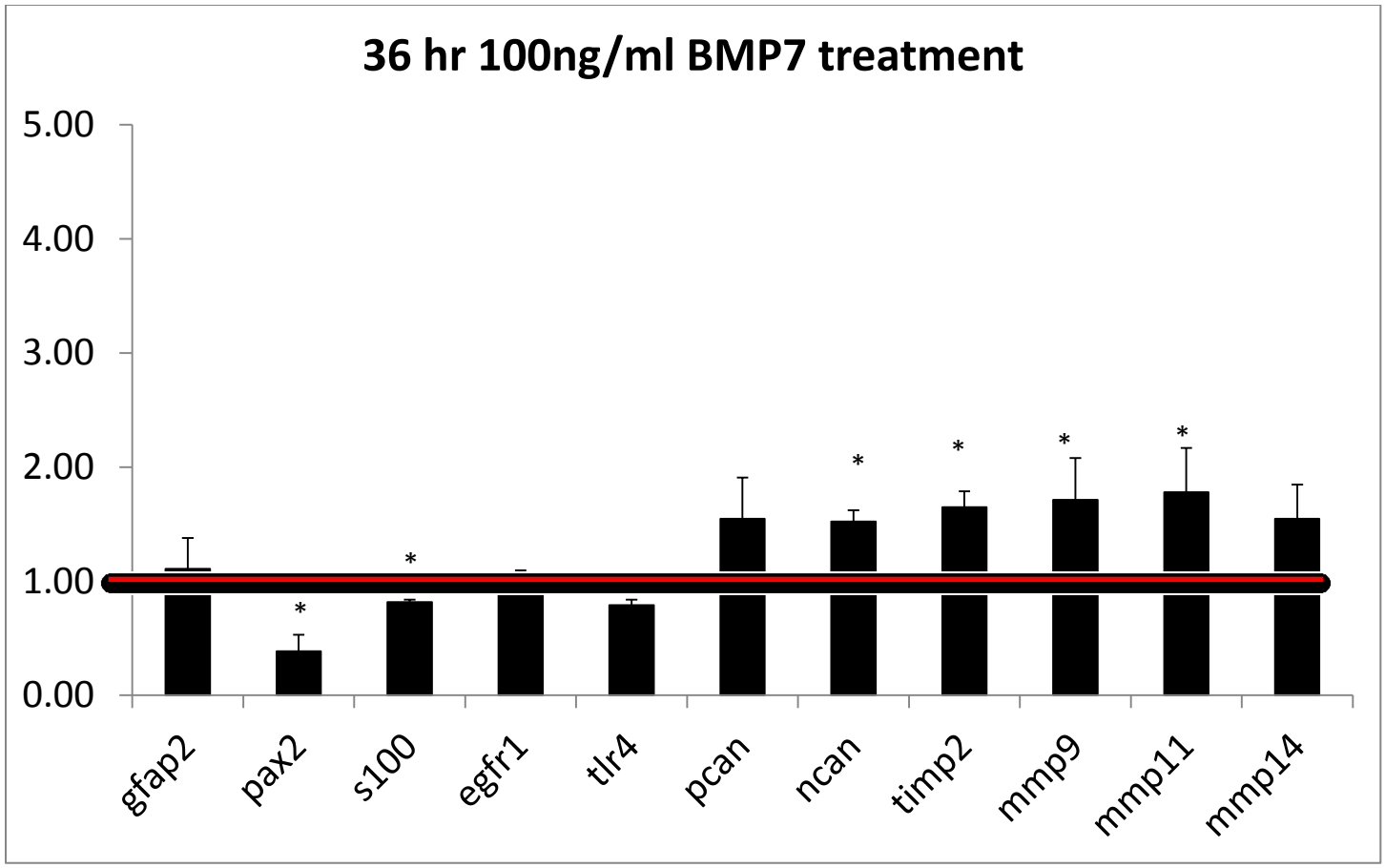

Fig. 21 **Effect of BMP7 on retinal astrocyte cells**: (B) qPCR data depicting markers which showed statistically significant change in levels of mRNA in astrocyte cells exposed to 100ng/ml BMP7 for 36 hours normalized to the control treatment (* = *p value < 0.05*)

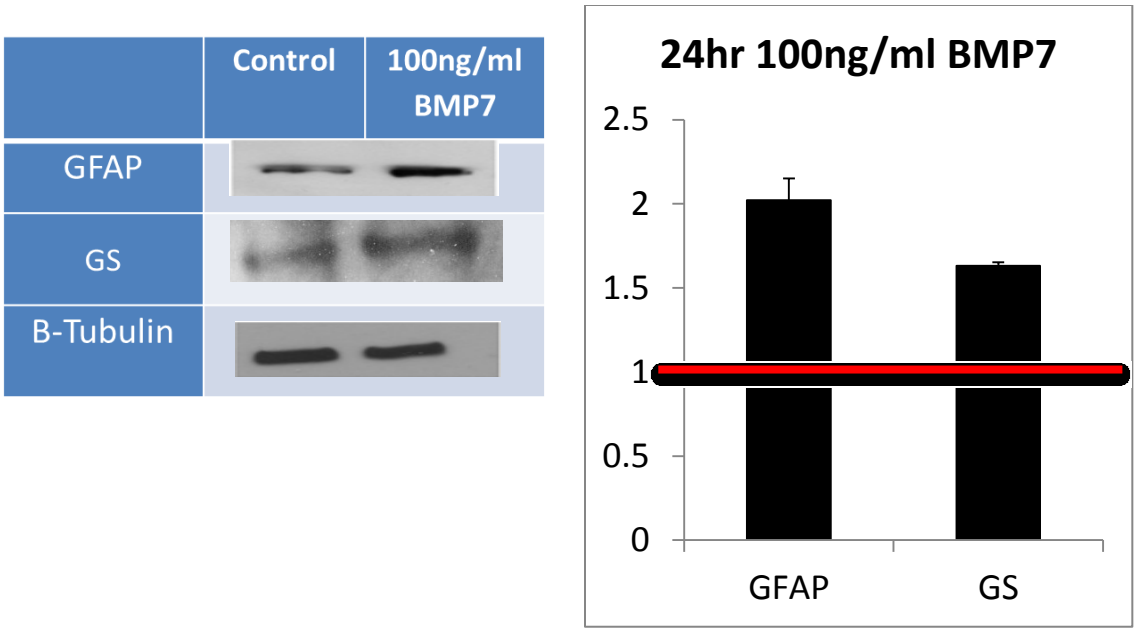

A. B.

Fig. 22 **Characterization of reactivity *in vitro* in BMP7 treated cells via western blot**: (A) Western blot analysis of 0.15mM peroxynitrite treated cells compared to the control treatments for GFAP, GS and beta tubulin (B). Densitometric analysis of the blots normalized to the control treatments. β-Tubulin used as the loading control

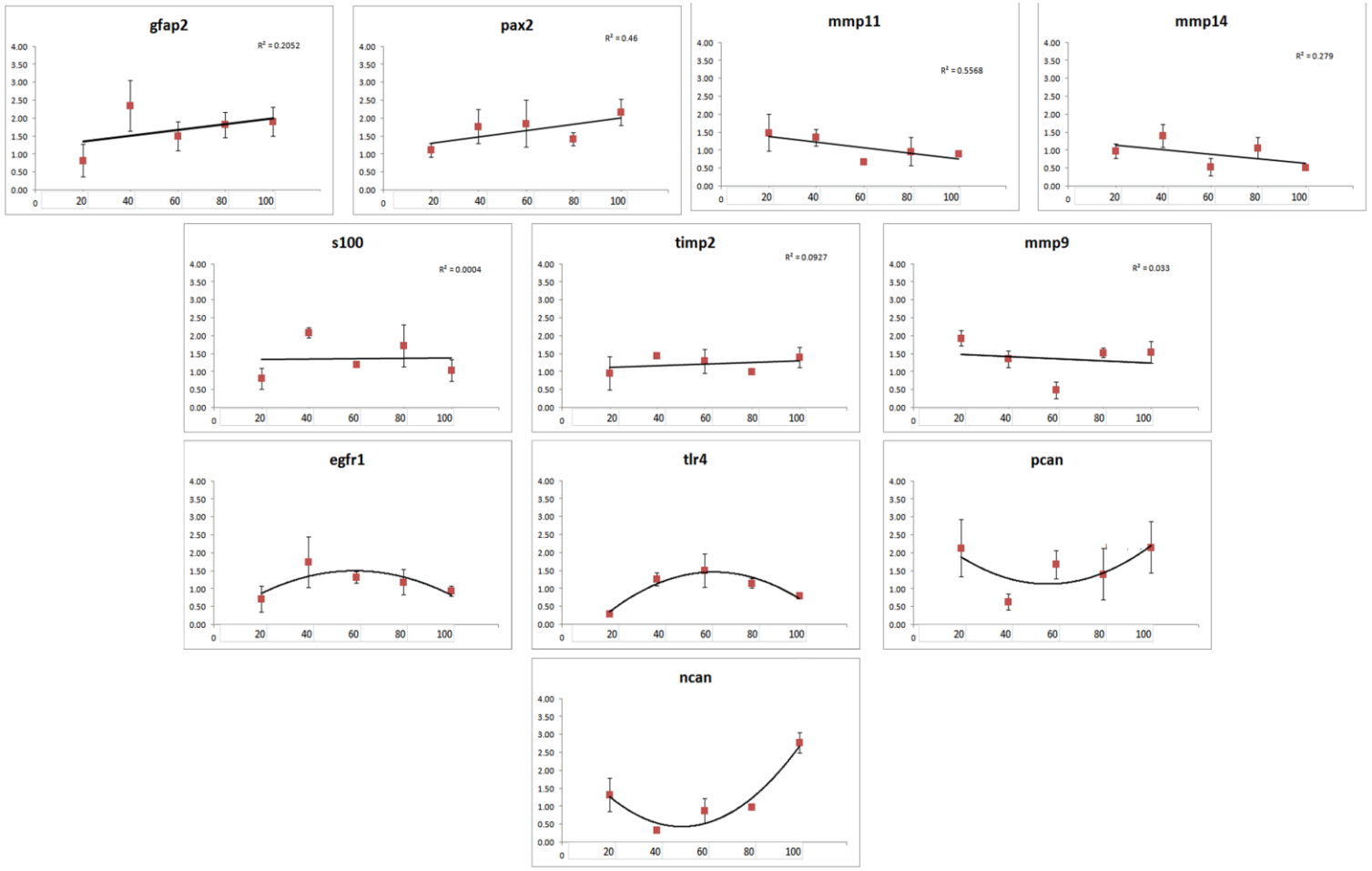

Fig. 23 **Effect of varying concentration of BMP7 on RNA levels of reactivity panel in retinal astrocyte cells**: Markers GFAP2, Pax2, MMP11 and MMP14 show a direct correlation with BMP7 levels, while S100, TIMP2, MMP9, EGFR1, TLR4, PCAN and NCAN show no or a complex correlation

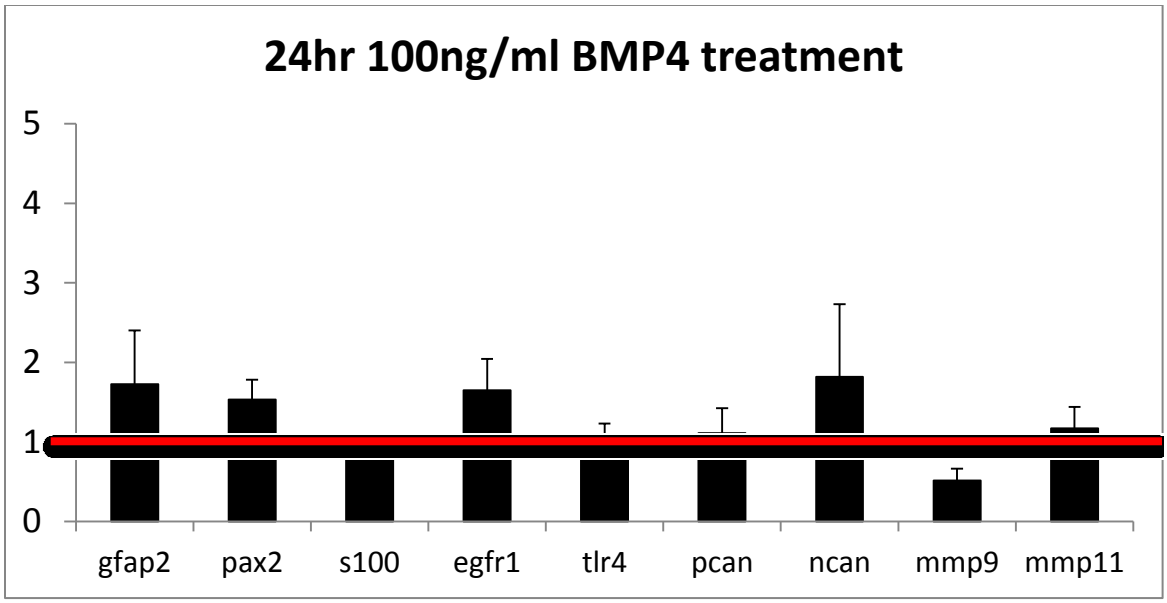

Fig. 24 **Effect of BMP4 on retinal astrocyte cells**: (A) qPCR data depicting changes in levels of mRNA of the reactivity panel of markers in astrocyte cells exposed to 100ng/ml BMP4 for 24 hours normalized to the control treatment

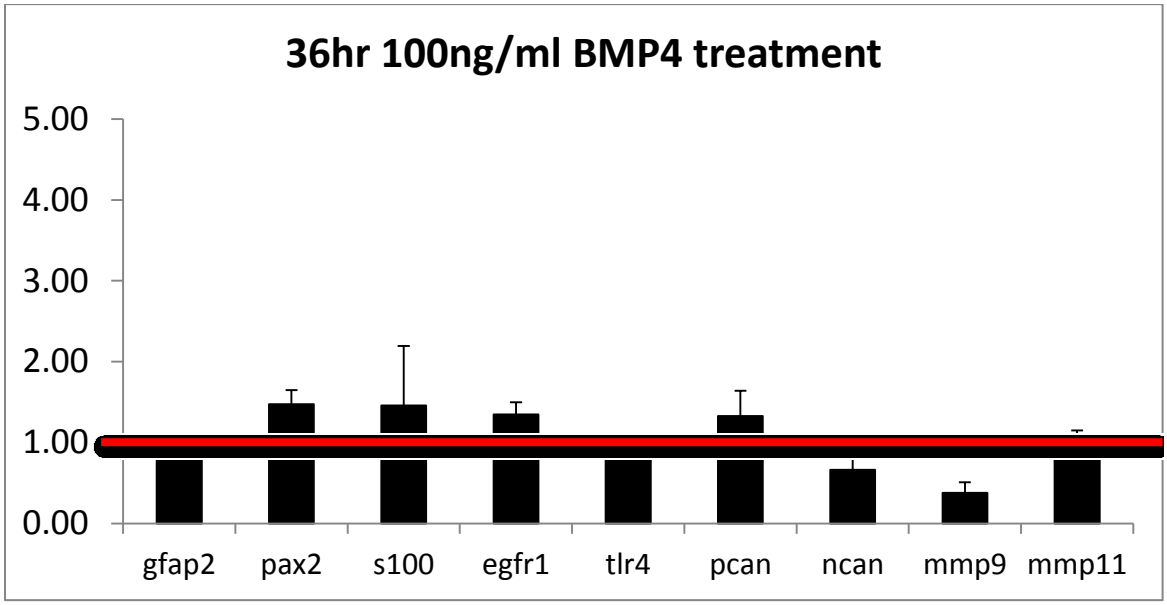

Fig. 24 **Effect of BMP4 on retinal astrocyte cells**: (B) qPCR data depicting changes in levels of mRNA of the reactivity panel of markers in astrocyte cells exposed to 100ng/ml BMP4 for 36 hours normalized to the control treatment

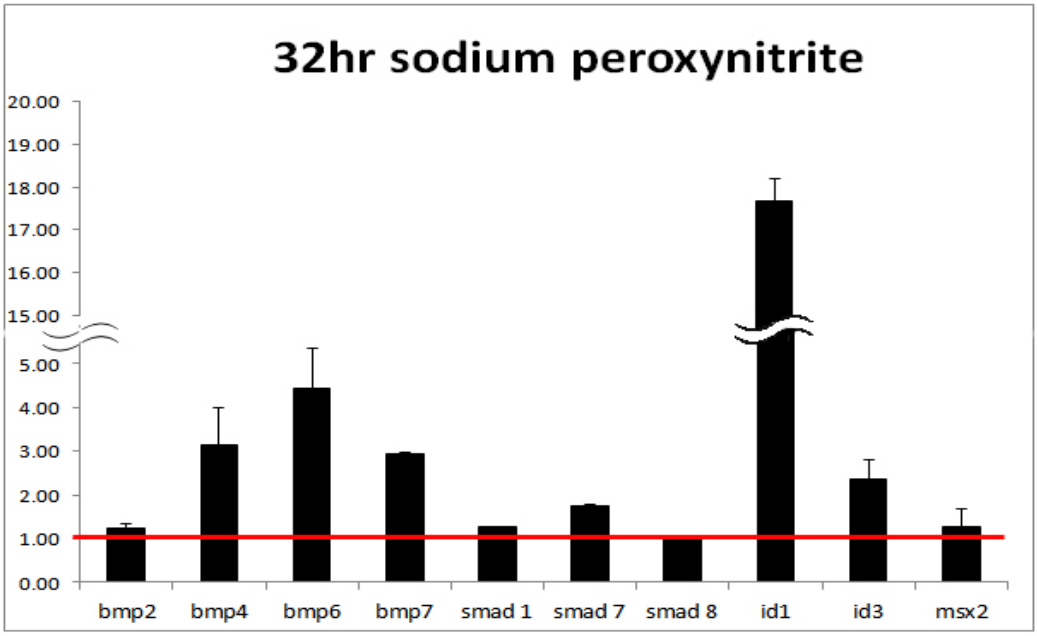

Fig. 25 **BMP molecules and signaling components *in vitro***: (A) qPCR analysis for levels of RNA for BMP molecules and downstream components of reactivity in 0.15mM sodium peroxynitrite treated cells, when compared to the control treatment condition

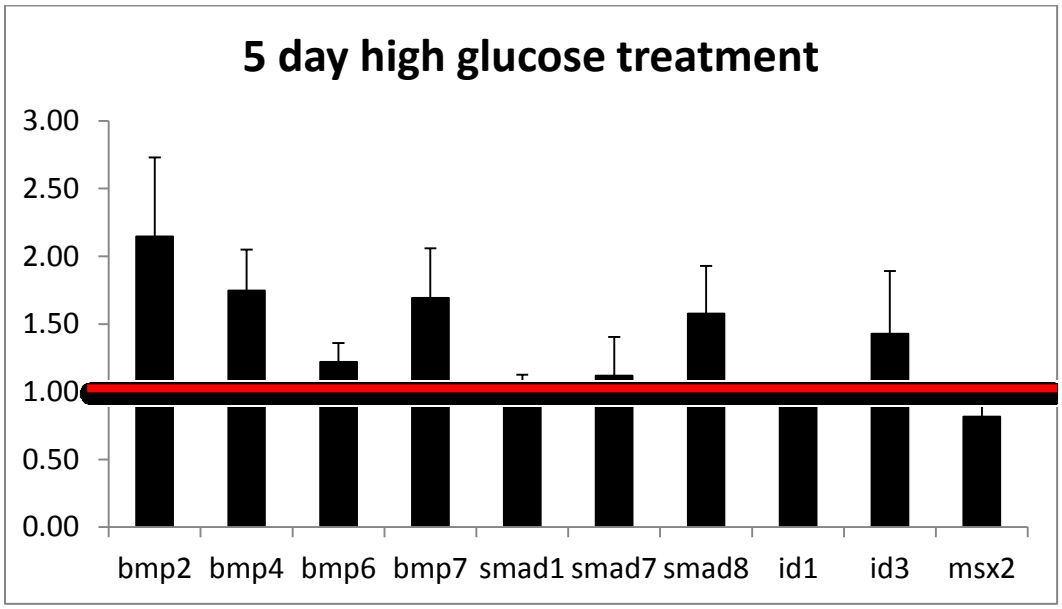

Fig. 25 **BMP molecules and signaling components *in vitro***: (B) qPCR analysis for levels of RNA for BMP molecules and downstream components of reactivity in 5 day high glucose treated cells, when compared to the control treatment condition

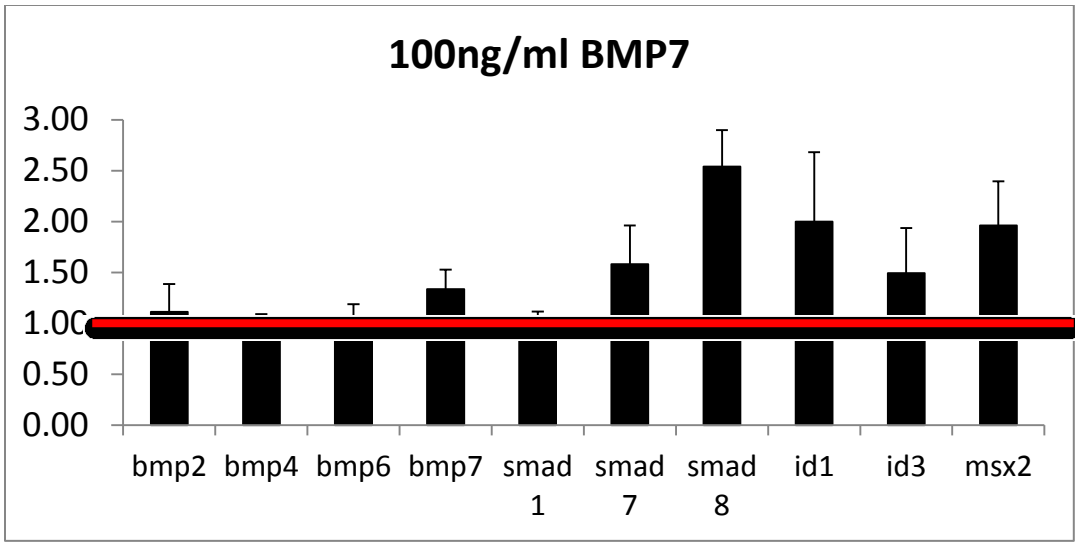

Fig. 25 **BMP molecules and signaling components *in vitro***: (C) qPCR analysis for levels of RNA for BMP molecules and downstream components of reactivity in 24 hour BMP7 treated cells, when compared to the control treatment condition

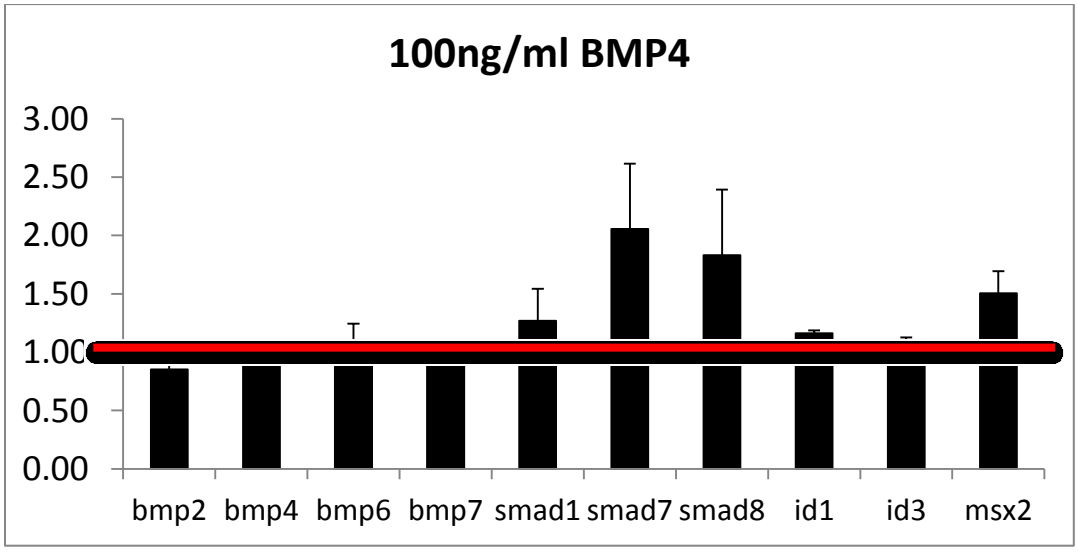

Fig. 25 **BMP molecules and signaling components *in vitro***: (D) qPCR analysis for levels of RNA for BMP molecules and downstream components of reactivity in 24 hour BMP4 treated cells, when compared to the control treatment condition

	pSmad1, 5, 8		B-Tubulin	
Treatment	Control	treated	Control	treated
BMP7	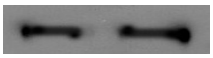		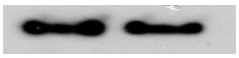	
0.15mM peroxynitrite	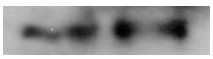		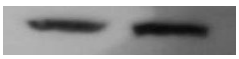	

A.

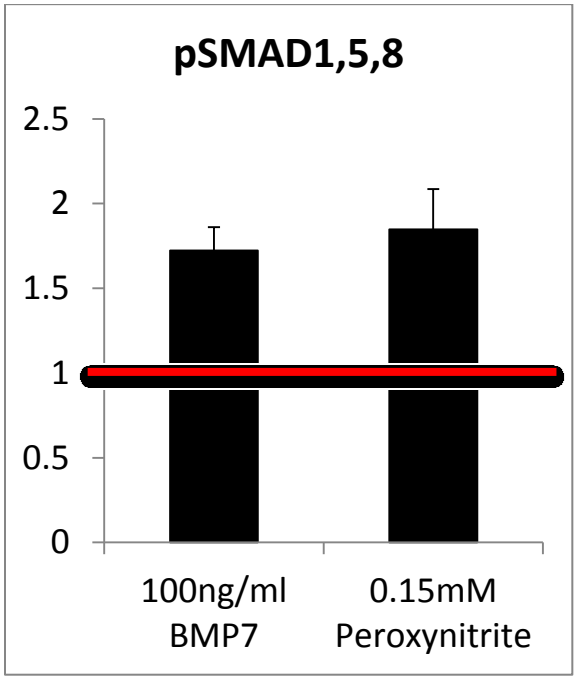

A.

Fig. 26 **BMP signaling in gliosis *in vitro***: (A). Western blot analysis of 100ng/ml BMP7 treated cells compared to the control treatments for GFAP and beta tubulin, showing similar increase in pSMAD levels in both BMP7 and peroxynitrite treated cells (B). Densitometric analysis of the blots normalized to the control treatments. B-Tubulin used as a loading control

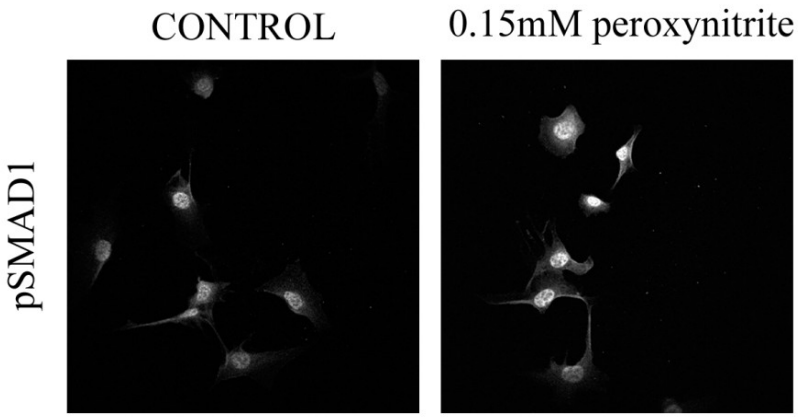

Fig. 27 **ICC for pSMAD activity in reactive gliosis *in vitro***: Immunocytochemistry of peroxynitrite treated cells with antibody against pSMAD1 which shows more intense nuclear staining in the peroxynitrite treated cells